INTEGRATED FLOOD MODELING IN LUBIGI CATCHMENT KAMPALA

HERVE VILLARD HABONIMANA
February 2014

SUPERVISORS:
Prof.Dr. V.G. Jetten
Dr.Ir. J. Ettema

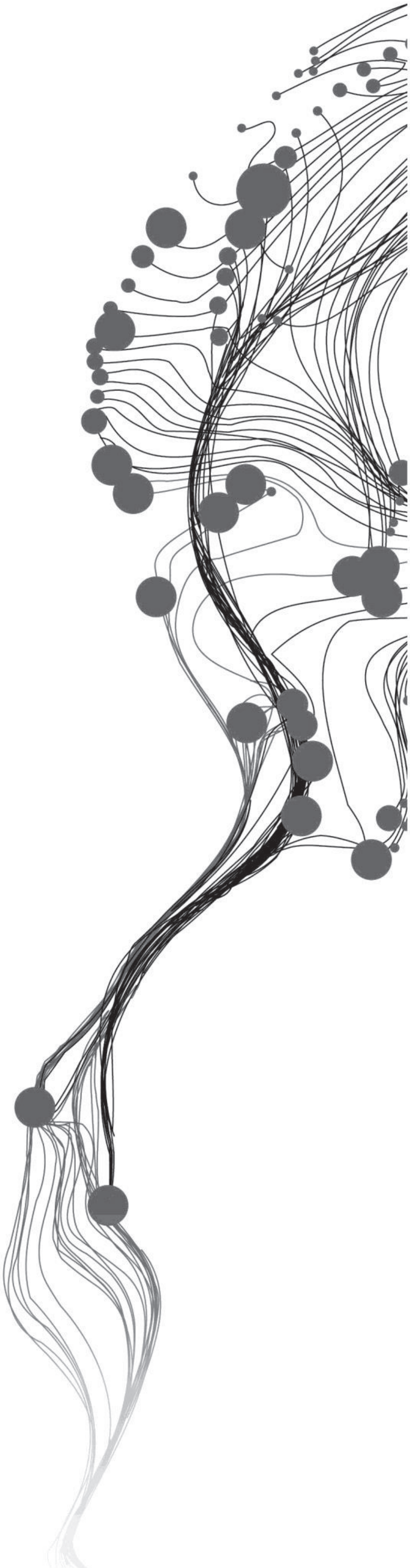

INTEGRATED FLOOD MODELING IN LUBIGI CATCHMENT KAMPALA

HERVE VILLARD HABONIMANA
Enschede, The Netherlands, February, 2014

Thesis submitted to the Faculty of Geo-Information Science and Earth Observation of the University of Twente in partial fulfilment of the requirements for the degree of Master of Science in Geo-information Science and Earth Observation.
Specialization: Applied Earth Sciences/Natural Hazards and Disaster Risk Management

SUPERVISORS:
Prof.Dr. V.G. Jetten
Dr.Ir. J. Ettema

THESIS ASSESSMENT BOARD:
Prof.Dr. V.G. Jetten (Chair)
Dr. R. van Beek (External Examiner, Universteik Utrecht)

Dedicated to my late parents
And
To my brother Kwizera and my sister Ishimwe.

ABSTRACT

Hydrological responses of urban catchment are highly sensitive to spatial variability of rainfall. However, spatial homogeneous rainfall is still the most predominant technique currently used in hydrological studies, especially in flood simulations. While relying mainly on the rain gauge measurements, the simulation underestimates the effect of spatial-temporal nature of rainfall events in hydrological response. The aim of the research was to integrate spatial-temporal variable rainfall of an observed extreme event into flood modelling, to analyse flood dynamics when rainfalls of different properties are used, to test the ability of OpenLISEM in flood simulation and to evaluate the performance of the model.

The study case was Lubigi catchment in Kampala city/Uganda. The catchment suffers from flooding events occurring every year and affecting a large number of the population, mainly poor, and threatening their livelihood. Flood evidences are numerous in Lubigi floodplains. Different coping strategies can be seen in every corner of habited floodplain where different structural measures were adopted. Some people elevate the ground level before the construction of their houses while the others will either put a barrier in front of doors or small dyke around the house, and small levee around drainage channels. However, lack of strong integrated flood management measures make any effort made by the population unsuccessful.

A rainfall event was defined as a period. Two rainfall events were considered different when the Minimum Inter-event Time MIT is above or equal to 60 minutes, total rainfall depth Ptot is superior or equal to 3mm, maximum rainfall intensity Imax superior or equal to 4mm/h, and duration D superior to 20 minutes. Over the period 14May 2012 to 11May 2013, 77 rainfall events occurred in the Lubigi catchment. The maximum intensity measured was 106.8 mm/h, the maximum duration was 5.5 hours, and maximum amount of precipitation fallen in one event was 66.2mm. The catchment received more rainfall in the afternoons of shorter duration while rainfall of longer duration occurred in the afternoons and that rainfall of higher intensities are relatively few. The total rainfall depth is stronger related to the maximum intensity than it is to the total duration. Only two rainfalls of two year return were identified among the records. The WRF model simulated the rainfall characteristics at a 1km spatial and 10-minute temporal resolution for the period 23 June to 29June 2012. Unfortunately, WRF model could not simulate the same atmospheric conditions that produced the 25th of June rainfall. However, WRF model simulated a major rainfall event the 27th of June. The 27June WRF rainfall was not in agreement with the measured rainfall either in space, amount, or duration. Some calibrations were performed to get similar maximum intensity and total rainfall depth as observed.

OpenLISEM successfully simulated different flood events for different rainfall inputs. The results were in terms of water available for runoff, total infiltration, peak discharge, total discharge, flood volume, flood duration, and flooded area. As expected, flood simulation using spatio-temporal variable rainfall led to different hydrological processes compared to when a spatial homogeneous rainfall was used. As WRF model simulated higher rainfall intensities in the north of the catchment, also higher hydrological responses are observed in the northern part of the catchment. It was obvious that homogeneous rainfall can underestimate/overestimate rainfall properties in areas without rain gauges, thus leading to erroneous runoff or flood estimation. However, simulation using homogeneous rainfalls can be more adequate in studying the flood risk in different parts of the catchment. The analysis of rainfall properties on flood dynamics showed that worse flood scenarios are produced by high intensities of short duration compared to longer duration with low intensities. Finally, a correlation test between simulated flood depth and measured flood depth from a field survey showed a reasonable level of agreement.

Keywords: Lubigi catchment, Rainfall event, WRF model, OpenLISEM simulation.

ACKNOWLEDGEMENTS

Many thanks to the Nuffic through a NICHE/RWA/071 project to fully finance my studies and for their effort to strengthen the capacity of the National of Rwanda to provide services of quality in the field of Geo-Information Science. I am thankful to the National University of Rwanda for providing me this opportunity to pursue higher studies.

Special thanks go to my supervisors Prof. Dr V.G Victor Jetten and Dr. Janneke Ettema for their admirable guidance. Without their wisdom, fruitful discussion, inputs and critical comments this thesis would not have been possible. I want to express my gratefulness to D.G Rossiter for providing soil data used for this research, Dr. John Wasige and Dr. Shuaib Lwasa of the University of Makerere for the assistance they gave during the fieldwork in Kampala, and ITC staff; Ir. Bart Krol, Drs. Nanette Kingma, and Dr. Dhruba Pikha Shrestha for advice and guidance.

I wish to thank my former supervisor Dr. Rwanyiziri Gaspard for encouraging me to study natural hazards and disaster risk management when I wanted to give up. I've learnt lots of things and got valuable knowledge through perseverance. Finally, this study would not have been easy without constant and valuable support from my family, my aunty Mukamurenzi in France, Rwandan community here in Enschede, and my classmates who made my stay in the Netherlands very pleasant.

Be blessed!

TABLE OF CONTENTS

LIST OF FIGURES

LIST OF TABLES

1. INTRODUCTION

1.1. Background

Flood hazards are affecting a large number of the population worldwide. Numerous flood events have resulted in losses of life, property damages, mass migrations, economic inflation, environmental degradation and even, disruption of societies (Jonkman, 2005; Roger, 2012). Floods alone killed about 100,000 persons and affected over 1.4 billion people during the 20th century worldwide (Jonkman, 2005), and loss attributed to flood are evaluated in millions of dollars with an exponential increase with time(Jongman et al., 2012). Also, statistics show that flood hazard is the most damaging among natural hazards and that cities are the most affected as most cities are in floodplains, preferred place for socio-economic development due to the development potential they provide. It is believed that the growing number of the world's population in general and physical development in floodplains particularly as highlighted are the main reasons behind the high physical and socioeconomic impacts of floods (Brody et al., 2008; Jongman et al., 2012; WMO, 2009).

Various researches have highlighted how urbanization processes also influence flood behaviour (Brody et al., 2008; Burns et al., 2005; Hollis, 1975; Li et al., 2013; Nirupama & Simonovic, 2007). They found that physical growth of urban areas, amongst others characterized by the increase of impervious surfaces leads to the decrease in infiltration rate thus to an increase of overland flow. A very modest rainstorm that earlier would be absorbed by soil storage in a rural catchment produces more surface runoff in an urban catchment. It might even lead to a flash flood due to fast and voluminous runoff water and the reduced time necessary for overland flow (WMO, 2009). That's why different flood protection and management initiatives have evolved in time as the population search for safety against flood (Kundzewicz, 1999; Kundzewicz & Takeuchi, 1999; Musgrave, 1985).

Flood management approaches have to consider all aspects of both flood behaviour and urbanization process. As Musgrave (1985), Kundzewicz and Takeuchi (1999), Kundzewicz (2002), Shrestha et al. (2011), and many others have highlighted, both structural and non-structural flood management approaches do exist. Structural methods focus on physical protection such as dikes, levees, dams, reservoirs, diversions, floodway, and channel improvements. Nonstructural methods concentrate more on flood warning and evacuation, watershed management, and insurance mechanism. However, none of the methods mentioned above guarantees an absolute safety against flooding (Kundzewicz & Takeuchi, 1999). Some methods just relocate the flood impacts spatially or temporally (WMO, 2009). Therefore, considering the limitations of existing methods, bringing together structural and non-structural approaches into Integrated Flood Management (IFM) is seen as the only way forward to reduce flood risk (Jha et al., 2012; Kundzewicz & Takeuchi, 1999; WMO, 2006, 2009).

IFM is a holistic approach which integrates different structural and non-structural flood management strategies together depending on the hydrological characteristics of a particular catchment (Hall et al., 2003; Jha et al., 2012). Thus, IFM activities rely on the knowledge of flood characteristics on a catchment scale like where, when, and why a given flood event happened. For this research, only two aspects of IFM were taken into consideration; rainfall properties analysis and flood modeling, mainly for two reasons. First, IFM uses modeling tools to determine the potential extent of flooding and helps identify and assess mitigation options. Secondary, recognize the source of water at catchment or basin level as very often areas affected by floods are sometimes far away from the source of water. Rainfall properties have been shown to highly influence flood dynamics on a catchment scale(Kusumastuti et al., 2007).

1.2. Rainfall data for hydrological models

Rainfall properties like total amount, intensity, duration and spatial distribution are highly important in hydrology and hydraulic studies. Bracken et al. (2008) showed that a spatial uniform rainfall of higher intensities on shorter duration leads to worse floods compared to the rainfall of long duration but with low intensities. But, in urbanized catchments, hydrological response is mainly marked to rainfall intensity. The effect of spatial and temporal distribution of rainfall properties also have been discussed by Faurès et al. (1995) and Patrick Arnaud et al. (2011). They showed that, beside a better representation of spatial variability of rainfall field, it influences not only the runoff volume and peak discharge, but also the shape of the hydrograph response in time. Effects of spatial temporal variability of rainfall can be expected to vary depending on the nature of the rainfall, the nature of the catchment, and the spatial scale of the catchment and rainfall (Segond et al., 2007).

The spatial variability of rainfall is one of the main sources of uncertainty in flood modelling (Patrick Arnaud et al., 2011; A. T Haile, 2010). While rain gauges are widely in use as a source of inputs to hydrological models, they suffer from a number of factors in accuracy measurements like design, precipitation phase, wind effects, evaporation or condensation as have highlighted Gruber and Lezivanni (2008). Additionally, low density of raingauges makes them unreliable in full rainfall field(Xie & Arkin, 1996). In order to overcome the spatial related issues, (Faurès et al., 1995) proposed the increase of raingauge density. However, as rainfall can vary on a very short distances and time(Kidd, 2001), it is almost impossible to have to reach required raingauge density. In the last decades, a number of alternatives have evolved with time like radar systems, Numerical Weather Prediction (NWP), and earth observation satellites to overcome the shortcomings of relying on rain gauges only. Nevertheless, radar systems and satellite rainfall have limited forecast skills as they cannot be produced prior to the rainfall event (Pennelly et al., 2014).

Numerical Weather Prediction (NWP) models allow researchers the ability to produce simulations reflecting either real data or idealized atmospheric conditions and can be used as input to hydrological model (Pennelly et al., 2014; Skamarock et al., 2008). In terms of flood risk, NWP is seen as tools for flood forecasters. One example of the NWP is Weather Research and Forecasting (WRF) model. Pennelly et al. (2014) verified the accuracy of the WRF Model in simulating heavy rainfall over Alberta, Efstathiou et al. (2013) analysed the sensitivity of WRF model on two commonly used boundary layer schemes by simulating rainfall over the Chalkidiki peninsula in northern Greece. They all have shown that WRF model is a reliable source of rainfall data. However, they also realized that different rainfall simulations using WRF model can result in overestimation or underestimation of measured rainfall event or displace it in space.

1.3. Flood models

Today, a multitude of flood dynamics models exists. Gareth and Sylvain (2007) reviewed some of the existing one-dimensional (1D) and two-dimensional (2D) flood models. Mostly these models share the dependency on the principle of conservation of mass, momentum and energy and can be based on finite elements or raster(Horritt & Bates, 2002). If the water is confined inside a river or any channel, it is best simulated as an unsteady 1D flow model (Stelling & Verwey, 2006) which solves a one dimension St Venant equations (Horritt & Bates, 2002). Such a 1D model defines flood only in terms of discharge and water level as a function of space and time. However, 1D models introduce errors and uncertainty in the simulation of overland flow, dam breach, flood extent analysis and evacuation plans as they are 2D in nature and they are best represented by 2D models (Horritt & Bates, 2002). 2D flood models predict flood inundation based on the 2D shallow water equations (Gareth & Sylvain, 2007; Mignot et al., 2006). The system of 2D shallow water equations consists of three equations: one equation for continuity and two equations for the conservation of momentum in the two orthogonal directions.

A more holistic coupled 1D/2D model is considered to give a better and accurate representation of physical processes of flood phenomena (Bamford et al., 2008; Lin et al., 2006; Vojinovic & Tutulic, 2009). Therefore, various models are now offering such capabilities; examples include SOBEK 1D/2D (Alkema, 2007), SW12D (Finaud-Guyot et al., 2011), LISFLOOD-FP and TELEMAC-2D (Horritt & Bates, 2002). However, some of these models do not fit well in IFM as they don't take into account the whole catchment but just focus of the flooded area. Thus, while many existing flood models might be defined as floodplain model, an integrated flood model should take into consideration both flood plain and upper catchment which is often the source of flood water in the context of IFM. Examples of software that offer flood modeling capabilities with a full coupled 1D/2D on catchment level include Flo-2D, LISFLOOD (Bates & Hervouet, 1999), and OpenLISEM (De Roo et al., 1996). In the context of IFM, this research will introduce an integrated 1D/2D OpenLISEM model which simulates floods by taking into account the whole catchment. OpenLISEM (the Limburg Soil Erosion Model) will be tested in flood simulations. Although OpenLISEM model was developed as an event based model for runoff/erosion in rural areas, recently a flood simulation extension was added. OpenLISEM can be used on urban or rural catchment on a scale varying from 10 to 100 km2. Evaluation of the capacity of the model in simulating floods in an urban environment is necessary.

1.4. Research problem

1.4.1. Flood simulation and rainfall variability

As discussed above, spatial variability of rainfall is very important in hydrology modeling and a single rain gauge as rainfall input carries great uncertainties regarding spatial runoff estimation (Faurès et al., 1995; Gruber & Lezivanni, 2008). There is a need of accurate representation of rainfall spatially and temporally for accurate estimation of runoff and thus flooding. Currently, flood simulations rely on spatial homogeneous rainfall without taking into account a full spatial-temporal domain that characterizes rainfall. This research will bridge that gap by using the rainfall simulated by the WRF model in flash flood simulations. Using OpenLISEM, an open source software for floods simulation, this research will analyse the differences in flood dynamics when using a homogenous or spatio-temporal rainfall.

1.4.2. Flash flood in Kampala

In their papers (Douglas et al., 2008)and Di Baldassarre et al. (2010) highlighted how cities and poor population, particularly in Africa, are being affected by flood impacts. Floods are causing widespread devastation, millions of people affected, loss of lives and livelihood, crops damaged, and thousands leaving their homes especially poor population who lives mostly in hazardous areas. Floods also lead to secondary hazards like mudslides, biological disasters like cholera (Matagi, 2002).

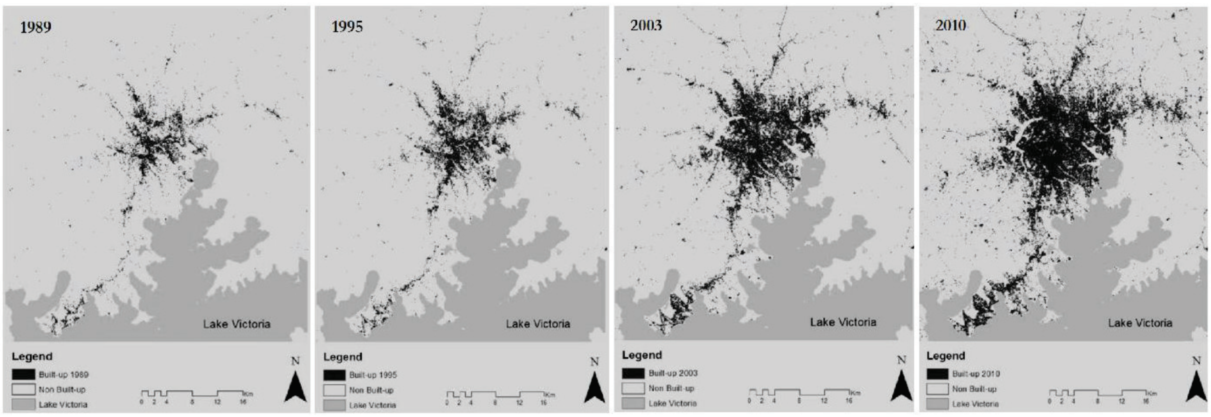

Figure 1.1: (Urban growth of Kampala city, from 1989 to 2010 (Abebe, 2013)

In Kampala, the capital city of Uganda, for various reasons floods are becoming more frequent and unpredictable (Douglas et al., 2008). Mainly poor population and their economic activities are affected every year by flash floods during rainy season (Jha et al., 2012; NEMA, 2008, 2010). In addition, Matagi (2002) and the National Environmental Authority of Uganda NEMA (2008) reported the increase in cholera, diarrhea and malaria diseases during floods.

In the last decades, the city has known an uncontrolled urban growth (Vermeiren et al., 2012). The unforeseen mass of migrants in search of employments caused the city to grow rapidly which resulted into an unplanned response to claims for low cost housing on hill slopes and wetlands (UN-Habitat, 2007). Floodplains, which use to be urban natural drainage systems (Matagi, 2002), then became occupied by slums mainly of poor population (Vermeiren et al., 2012). It is believed that the urbanization reduced the rainfall infiltration capabilities and increased runoff to six times than was in natural environments

(Douglas et al., 2008). Other causes of floods include; drainages which are poorly maintained, sometimes filled with silt, and limited to major roads (UN-Habitat, 2007), the nature of rainfalls which are characterised by high intensities (Matagi, 2002).

Currently, less is documented in the state of flooding in relation to the contribution of the urbanization process in Kampala and rainfall characterizing the area. In the context of IFM and using an integrated flood model, this research will analyse floods in Lubigi catchment in relation to dominant rainfall event properties. The upper part of the Lubigi catchment (28 km2) is located entirely within the city and is considered representative of several such catchments where flash floods occur in Kampala.

1.5. Research objectives

The main objective is to analyse rainfall properties of Lubigi catchment, to integrate spatial and temporal variability of rainfall data in a flood model, and to analyse the effects on fluid dynamics.

1.5.1. Specific objectives and research questions

i. To analyse rainfall events characterizing the catchment and include their spatial and temporal characteristics.

- *What are the best ways to characterize a rain event?*
- *What is the relationship between different rainfall characteristics?*
- *How does the ground measurement relate to the prediction of WRF?*

ii. To model different flood events using OpenLISEM.

- *What are the floods' evidences in Lubigi catchment?*
- *What are the differences or similarities between flood simulated by homogenous rainfall and the spatio-temporal variable rainfall?*
- *What is the change in flood behaviour with different rainfall characteristics in relation to soil infiltration?*
- *Do the simulations relate to the reality of the floods in the catchment?*

2. STUDY AREA

The study area is located in Kampala, the capital city of Uganda a country in the central eastern part of Africa (Figure 2.1). The city of Kampala is around 0°15N and 32°30E, 45 km north of the Equator. Lubigi catchment occupies the northwestern part of Kampala city. Like other parts of the city, Lubigi catchment is made by hill and low lying valleys with elevation varying from 1154 and 1306 above sea level and with slopes varying between 0 and 45 degrees as shown in Figure 2.2.

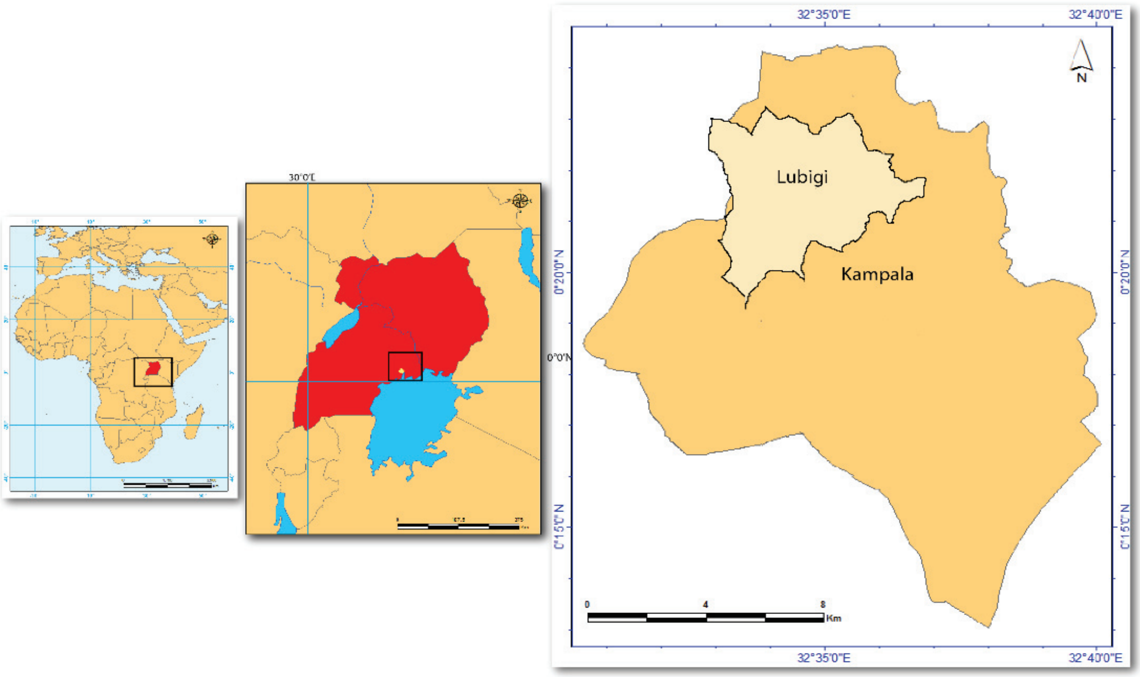

Figure 2.1: Uganda and its location in Africa, including the location of Kampala inside Uganda with Lubigi catchment located in the northern west.

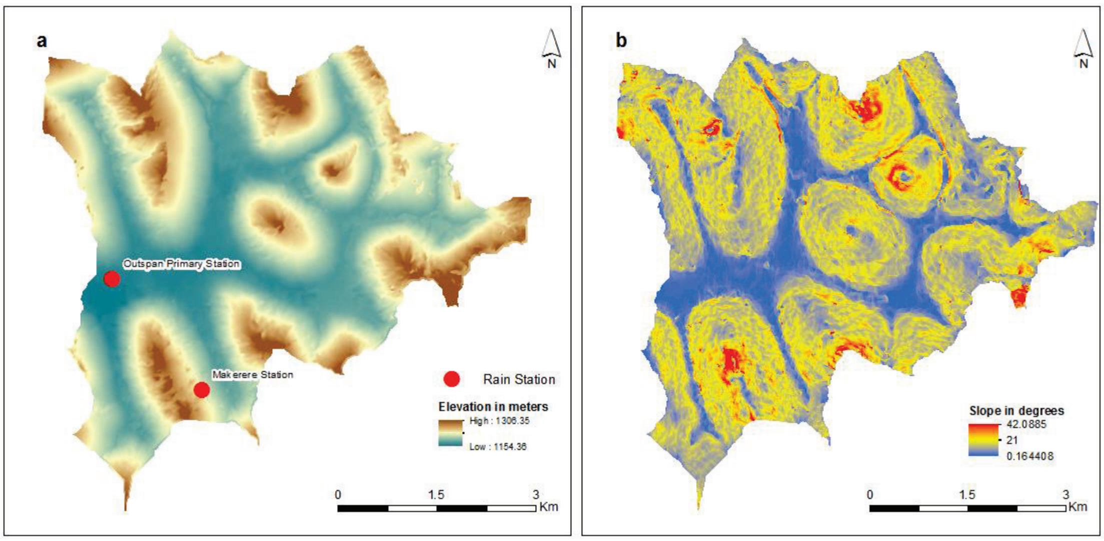

Figure 2.2: (a) Elevation map in meters with the location of two rainfall stations used in the research and (b) slope maps both for the Lubigi catchment.

2.1. Climate

The climate of Uganda like other countries of East Africa is highly influenced by Inter-Tropical Convergence Zone (ITCZ) (Maidment et al., 2013; Philippon et al., 2002), and East and South East monsoons according to NEMA (2009). In addition, altitude, North-East and South East monsoons, and water bodies play a major role in dictating local variability of rainfall (NEMA, 2009). Water bodies dominate local variation of precipitation, which is explained by highest annual average of rainfall found around the major lakes in Uganda as can be seen in Figure 2.3 (Maidment et al., 2013). According to Maidment et al. (2013), The southern part of Uganda including Kampala has two distinct rainfall seasons (February to June and August to November) coinciding with the northward and southward passage of the ITCZ. Kampala city, and the study area, are located in Lake Victoria basin climatic zone, which receive between 1200-2000mm per year (NEMA, 2009). Matagi (2002) stated that the annual rainfall average was 1200 mm and that rainfall in Kampala is mostly thundery characterised by heavy high intensity rainfall over short periods. Detailed analysis of rainfall characterising Kampala can be found in the report done by (ACE, 2010).

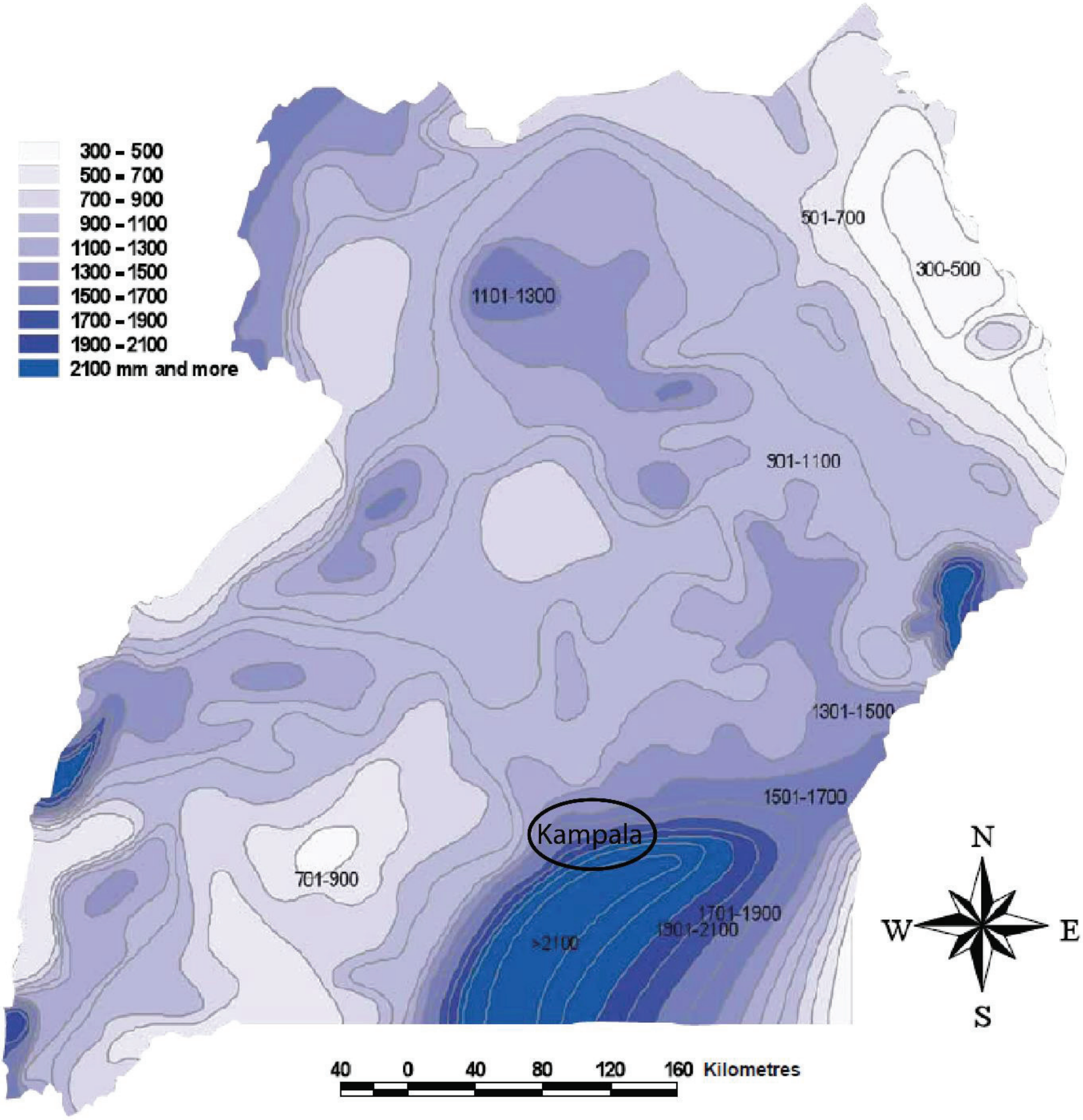

Figure 2.3: Average annual rainfall distribution in mm over Uganda. Source: (NEMA, 2009)

3. METHODOLOGY

3.1. Overview

The aim of this research is the integration of spatial-temporal rainfall data in flood simulation and evaluation of OpenLISEM in flood simulation. The research is divided into three parts as summarized in Figure 3.1 to address specified research questions. The first part focused on baseline data preparation to be used as input in flood simulation. These data include rainfall data, soil data, and flood survey's outcome. The second part focuses on OpenLISEM flood simulation using homogeneous rainfall and spatio-temporal variable rainfall. The third part compared the result of different flood simulations and with the outcome of the survey. This chapter gives in details methods and tools used.

3.2. Data collection

In order to assess the dynamics of a flood event several sources of information are essential. As this study uses OpenLISEM as the main tool for flood simulation (described later in section 3.3), the focus of data collection is on the input fields required by this model (Table 3.2). Some of the data were already available. A 5 by 5m Digital Elevation Model (DEM) represents the true ground surface, which is the principal variable that affects the movement of the flood. Classified land cover maps from Geo-eye images of 2010 of the city with 0.5 m spatial resolution is used. Rainfall records provide daily rainfall at two stations up to 2007 and detailed rainfall records in 10 and 15 min intervals since May 2012 at Makerere University and Outspan Primary School. Additionally, Ettema simulated rainfall using WRF model on a grid of 1 km spatial resolution covering the whole of Kampala with 10 minutes temporal resolution the period 26 – 30 June 2012. Soil data have been collected by Dr. D.G Rossiter in September 2013 to provided information on hydraulic conductivity, porosity, and depth of the soil characterizing the catchment. The author conducted a field survey was conducted from 27th of September and 19th of October 2013 to collect data related to the drainage systems and flooding in the catchment through metric measurements and stakeholder survey.

Type of data	Method	Source
Topographic data (5x5m)	Derived from DEM	KCCA
Land cover	Obtained from image classification	Done by Mhonda/former ITC Msc student;
Rainfall	Measurements by rain gauges	Makerere University and Outspan Primary School/ meaured
	Modelled spatial rainfall	WRF operated by Dr. J. Ettema /ITC
Drainage system	Manual drainage system measurements	Fieldwork
Soil information	Laboratory measurement of undisturbed soil samples	Done by Dr. D.G Rossiter/ITC
Flood depth	Metric field measurements of past flood events	Fieldwork

Table 3.1: List of collected data with the methods used including the source.

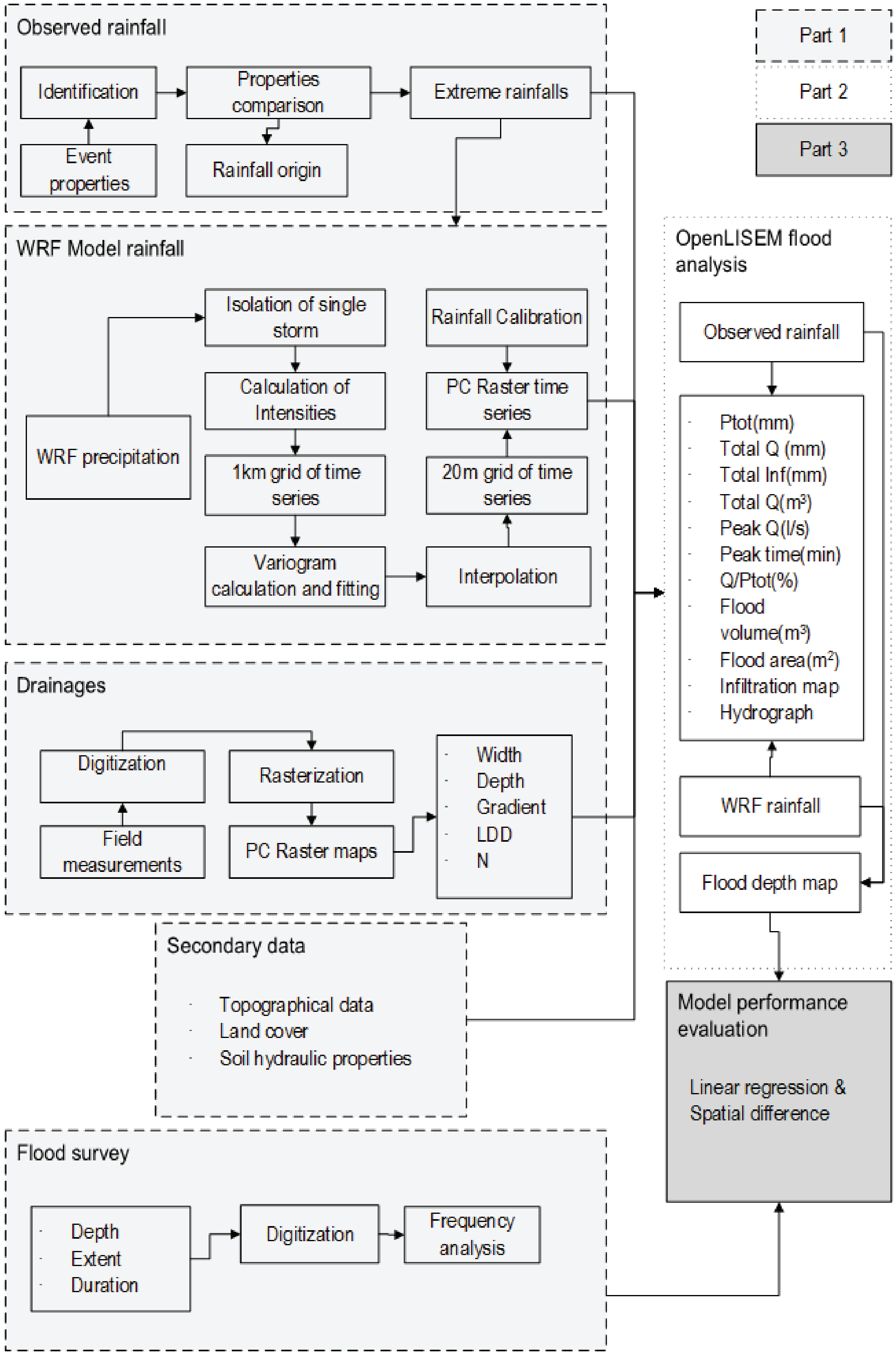

Figure 3.1: Flowchart of the methodology. The research relied on three main parts; Part 1: baseline data preparation, Part2: OpenLISEM flood analysis, and Part3: Model performance evaluation. The abbreviations in the figure are explained further in the text.

3.2.1. Rainfall data

Ground station measurements

Two automatic rainfall stations (Figure 3.2) have been installed in the catchment, the first the 22 of April 2012 at Makerere University (0˚20'5N, 32˚33'59E) and the second in June 2012 at Outspan Primary School (0˚21'2N, 32˚33'29E). They both collect high resolution rainfall data at 10 minute and 15 minutes time step. However, some data presented gaps in records due to receiving device or people in charge of downloading the data. Thus, the outputs of the two stations were combined together for analysis.

Single rainfall events have been isolated from observed of the combined records. The characteristics of a rainfall event to be considered as a single event are difficult to define. But, most consider minimum inter-event time (MIT), event duration D, maximum rain depth Ptot, maximum intensity Imax, average intensity $\bar{I}$ (Brown et al., 1985; A. T. Haile et al., 2011). Here we follow the approach of Brown et al. (1985) and (A. T. Haile et al., 2011), where a single event is defined as a period. According to Brown et al. (1985) total duration (D; min), total precipitation (Ptot; mm)[1], and maximum precipitation intensity (Imax; mm/h) [2] are the most important rainfall event characteristics that highly influence flood dynamics. Thus, in the present research we focused on these three characteristics when identifying a single rainfall event.

In order to analyse the single rainfall following the approach of Brown et al. (1985) and A. T. Haile et al. (2011), a single primitive rainfall events were defined as a period of D≥20 , Ptot ≥ 3mm, Imax ≥ 4mm/h, and MIT≥60min which is the length of dry period (A. T. Haile et al., 2011). Thus:

$$P_{tot} = \sum_{i=1}^{D} P_i \qquad [1]$$

Where Pi is 1min rainfall depth at ith minute and D the event duration. Imax is calcurated for an aggregation of t minutes as follows:

$$I_{max} = \max_{1 \le t \le D}\left(\frac{60}{t} P_i\right) \qquad [2]$$

where max indicates the maximum whereas the value 60 is used to change t-minute rainfall depth to hourly rainfall intensity (A. T. Haile et al., 2011).

Following the example given by Andy (2009) for analysis of nonnormal distributed data, a bivariate correlation using Spearman's rank r correlation defined as:

$$r = 1 - \left(6\sum d^2 \Big/ n \quad n^2 - 1 \right) \qquad [3]$$

was used to investigate n numbers of pairs of rainfall event characteristics with d the difference between two numbers in each pair of ranks.. This allowed checking empirical relationship between rainfall properties. In addition, daytime of rainfall was an important factor in order to know the origin of rainfall. Finally, extreme rainfall events identified in relation to the outcome of the research done by (ACE, 2010) on the return period of rainfall in Kampala were used in flood simulation.

WRF Model rainfall interpolation

The ground stations provide only high temporal resolution local point measurements, while accurate estimates of rainfall intensity distribution with high temporal and spatial resolution are necessary in most urban hydrological studies. Especially, urban hydrology requires rainfall measurements with high temporal and spatial resolutions (Berne et al., 2004). The Weather Research Forecast (WRF) model is seen as an alternative as it simulates rainfall events with high temporal (10 min) and spatial resolution (1km).

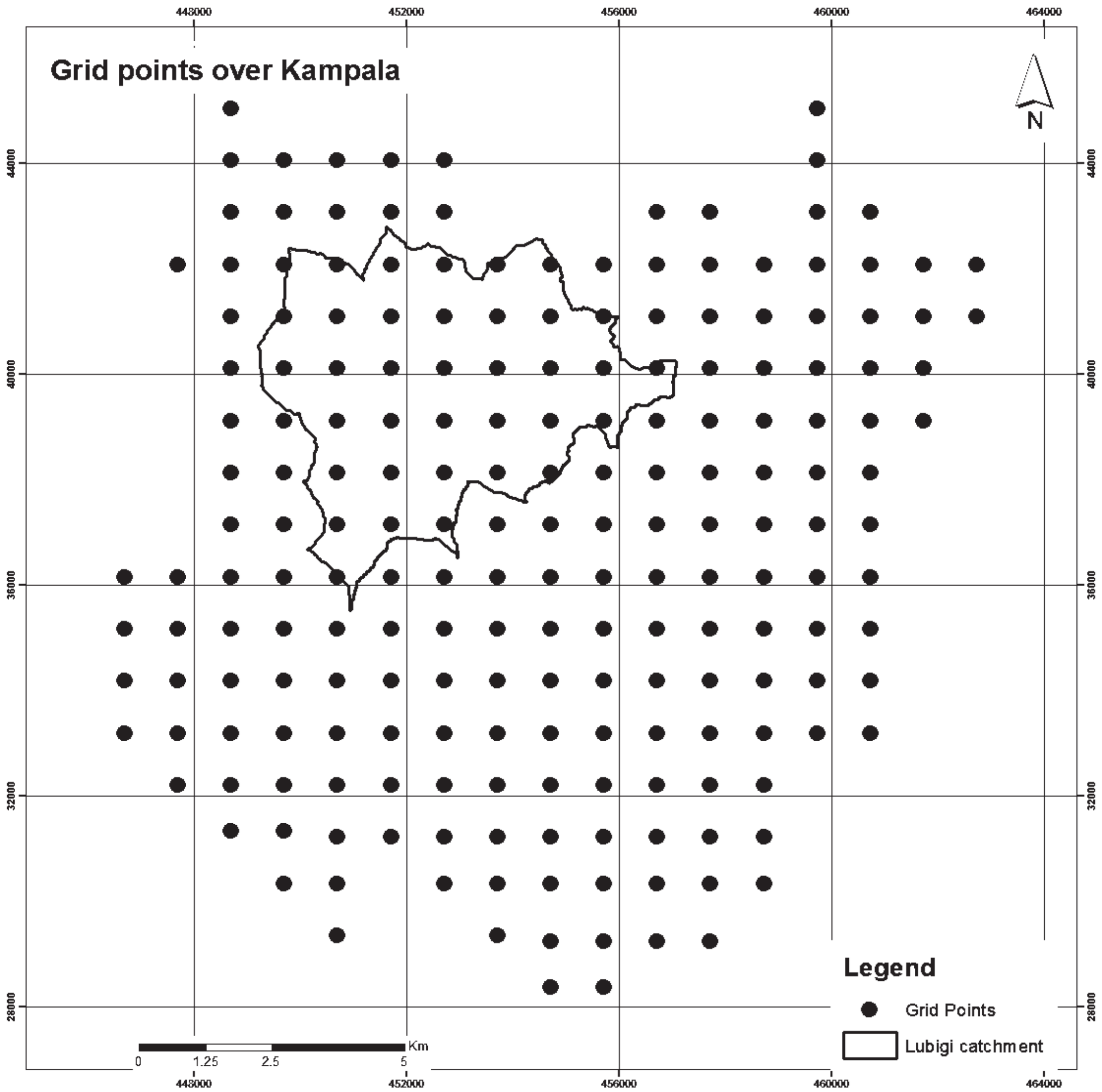

Figure 3.2: WRF model grid over Kampala (1km). The outline in the upper left corner is the Lubigi catchment boundary

The WRF model domain extends far beyond the boundaries of the Kampala region in order to simulate the physical processes related to precipitation accurately. In Figure 3.2 the regular model grid point distribution over the Kampala region are shown by the black dots. Accordingly 32 grid points are located in the Lubigi catchment, which are used for this study. Scaling down to 20 m spatial resolution was required to meet the resolution requirements of OpenLISEM through interpolation. Spatial correlation for every time step was modelled by the semivariograms that measure statistical correlation as a function of distance. The semivariance γ(h), calculated using Gstat package (Pebesma, 2013) of R which handle spatial statistical modelling, is defined as:

$$\gamma \; h \; = \frac{1}{2N_h}\sum_{i=1}^{Nh}(Z(s_i) - Z(\mathrm{s}_i + h))^2, \forall h \in h, \qquad [4]$$

Where γ(h) is be estimated from N_h number of point pairs *Z(Si) , Z(Si+h)* separated by a vector *h* (Bivand et al., 2013). The spatial prediction relied on different semivariograms models; spherical [5], exponential [6], Gaussian [7], and Bessel [8] where c is the sill, a the range and K1 the modified Bessel function of the second kind of order one. Ordinary Kriging (OK) shown in eq. [9] was chosen for this research because OK and Inverse Distance Weighting (DW) are considered to be the best methods as they provide smaller RMSE value in geostatistical interpolation of rainfall data (Ly et al., 2011). Ź is the predicted rainfall depth at the point Z0 as a weighted average of the rainfall depth values at all sample points xi, λi is the weight assigned to the sample point. No other influence took into consideration so far, like topography, wind direction because they are used as input to the WRF model during the simulation (Skamarock et al., 2008). Thus, these effects are already contained in the simulated data.

$$\gamma(h) = c\left(\frac{3h}{2a} - \frac{1}{2}\left(\frac{h}{2}\right)\right) \text{for } h \le a, \quad \text{for } h > a \qquad [5]$$

$$\gamma \quad h \quad = c \quad 1 - e^{-h/a} \quad \text{for } h \ge 0 \qquad [6]$$

$$\gamma(h) = c(1 - e^{-(h/a)^2}) \text{for } h \ge 0 \qquad [7]$$

$$\gamma(h) = c(1 - a.h.K_1(a.h)) \text{for } h \ge 0 \qquad [8]$$

$$\acute{Z}(z_0) = \sum_{i=1}^{N} \lambda_i z(x_i) \qquad [9]$$

The WRF produces 10 min timestep rainfall on the 1 km grid, and the variogram fitting and geostatistical interpolation was repeated for every timestep separately.

3.2.2. Drainage channel measurements

Characterisation of the entire drainage system is essential for accurate modelling of the flood dynamics as OpenLISEM simulates floods when runoff water exceeds channels or drainage systems. Due to incomplete ground data measurements, the focus during fieldwork was extending information of the primary and secondary drainage systems in the Lubigi catchment. Measurement of top width, bottom width, and depth of drainage channels were taken using BOSCH PLR 50 Laser Rangefinder and the 8 metres measuring tapes. In addition, the type of the materials that compose the bed and banks of drainage channels were recorded in a notebook as they are the most important factors that affect the choice of manning's n values which is roughness coefficients that reflect the resistance to water flows in channels (Arcement et al., 1984). Figure 3.3 (a) show all 269 points measured along existing drainage channels or new drainages.

3.2.3. Flood information survey

Usually, the performance of flood models is tested by relating the observed flood extent and duration to the predicted flood extent and duration. For this research no observed information was available. A participatory approach was used for getting information about flood depth and duration along different transects in areas reported to have experienced floods. As shown on the Figure 3.3 b, it was not possible to follow a transect due to the urbanization style of the area. Most of the targeted respondents live in wetland or in the lowland areas (Figure 3.3 b). The information was gathered by asking local population and measuring physical evidences. Only respondent living in the area for at least one year were considered because we assumed that their information would be reliable. The results were to be compared with the output of the model different transects in the floodplain were to be followed. The questionnaire asked can be found in the Appendix 7.1. Important questions related to flood awareness of the population before coming to settle in the area, the average flood occurrence in a year, the average duration of one single flooding event, and the protection measures. Taking flood depth measurements was very challenging in terms of accuracy and reliability of respondents.

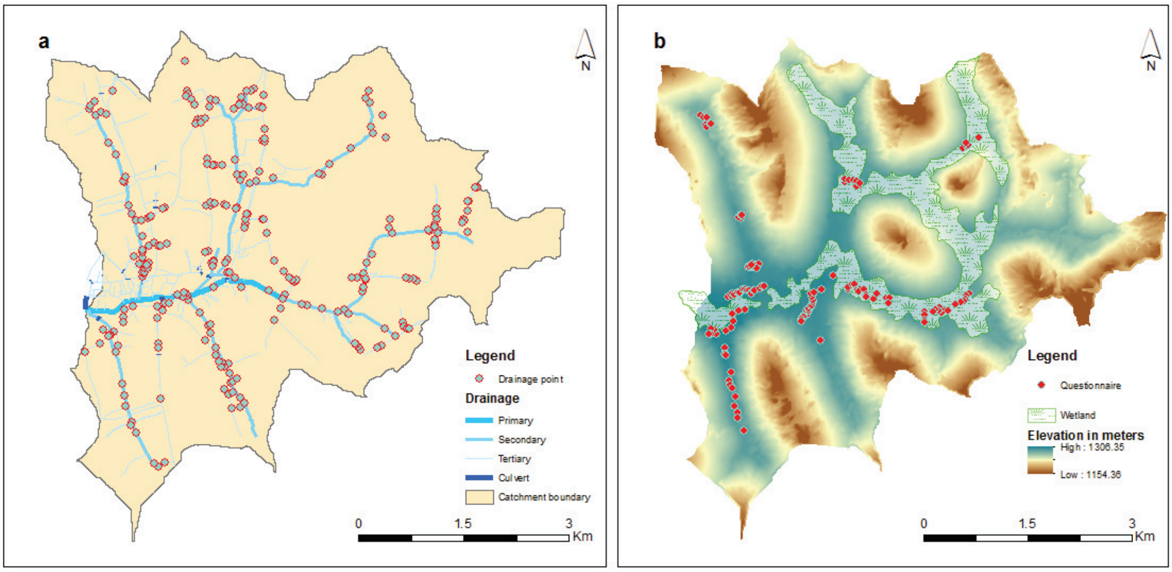

Figure 3.3: (a) Field measurements of drainage channel properties (b). Questionnaire survey places with the former assumed wetland.

3.3. Flood simulation

3.3.1. OpenLISEM model

OpenLISEM is an open source software that was used in this research to simulate flood dynamics of Lubigi catchment. OpenLISEM is a raster and event based model that simulates the surface water and sediment balance for every gridcell with spatial and temporal details. The model can be used to analyse the effects of land use changes or watershed management measures on runoff, flooding and erosion on a single rainfall event (Jetten, 2013a). OpenLISEM was developed first as runoff and soil erosion model for planning and conservation at the catchment scale (De Roo et al., 1996).

The Figure 3.4 shows eight main components of OpenLISEM related to flood simulation. In 1D domain, OpenLISEM calculates on the grid level the rainfall (mm/h), interception (mm), infiltration (mm/h), and surface storage. In the spatial domain, OpenLISEM calculate runoff and channel flow and shallow flooding from the channel system (Jetten, 2013a). OpenLISEM uses rainfall of high spatial and temporal resolution. Input rainfall data can be in the form of raingauge networks with their influence zones or rainfall intensity maps (Satellite, radar). The infiltration f is assumed to be depending on gravity and the suction of the wetting front. For every timestep a potential infiltration fpot rate is calculated and compared to the rainfall intensity. If the infiltration rate is larger than the rainfall intensity, the actual infiltration rate is equal the rainfall intensity else equal to fpot. For this research, OpenLISEM calculated rainfall the infiltration based on Green & Ampt equations. Additional details on surface storage and interception can be found in (Jetten, 2013b)

In the spatial domain, flooding in OpenLISEM follows a 1D/2D approach. Runoff water is accumulated on a predefined flow network with a kinematic wave procedure. The flow network is provided by the user and is usually based on the flow direction in a 3x3 cell window following the steepest slope. The kinematic wave converges water to a single outflow point where it leaves the catchment. The kinematic wave is an iterative procedure using the user defined timestep of the model, which is usually in the order of 5-60 seconds. Furthermore, it is possible to define a channel network, for manmade channels or natural riverbeds. In cells which contain a channel, part of the runoff water is diverted to the channel, and the channel captures rainfall directly. The amount of water reaching the channel depends on the runoff velocity, the timestep and the size of the gridcell compared to the channel size. The channel characteristics are defined by a series of maps for width, depth, bed slope angle, channel wall angle, manning's n, and cohesion. The channel can be made impermeable or can infiltrate water. Once there is water in the channel, the kinematic wave is executed a second time for the channel alone, using a channel network map, to route the water to the outlet.

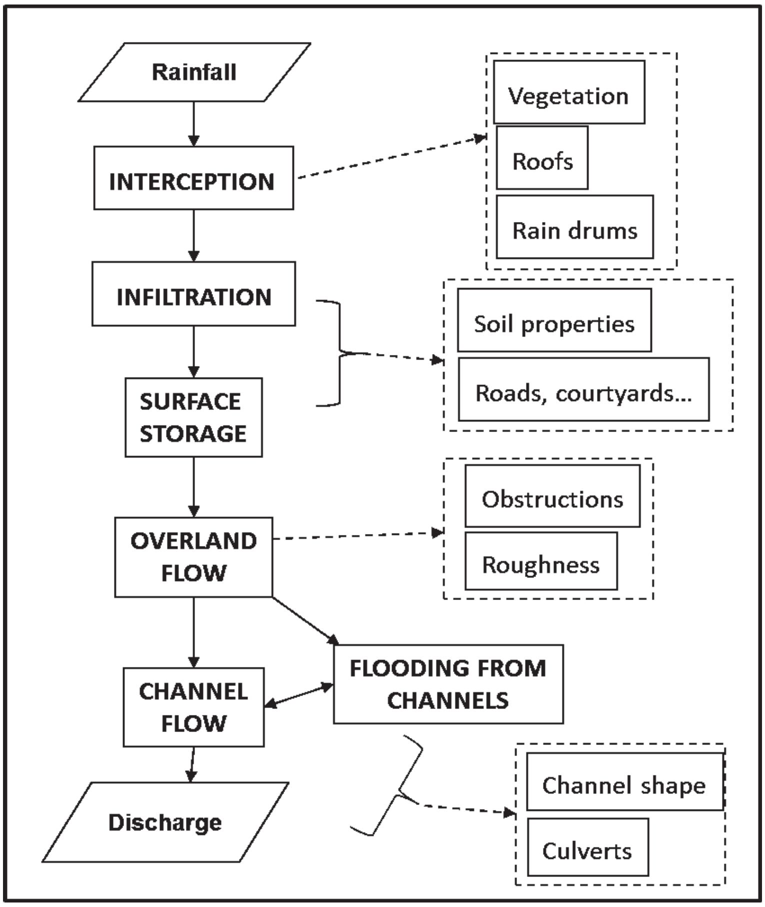

Figure 3.4: Simplified flowchart of OpenLISEM with the main variables needed as maps.

Finally, when the discharge wave reaches a height that is larger than the channel depth, the water overflows back onto the adjacent surface. Depending on the amount of overflow, substantial flooding can take place. The flooding is done using an opensource "FullSWOF" method proposed by Delestre et al. (2009) based on the classical system of Saint-Venant equation for shallow water floods. The term shallow in this case refers to the assumption that the flooding can be estimated with one average flow velocity and does not need to take vertical velocity changes into account. The method uses an explicit numerical solution with a varying timestep, where the timestep is adjusted to meet stability criteria. The method is fast and robust with a high precision. The flood module is executed as many times as needed to "fill up" an OpenLISEM time step. Typically, an OpenLISEM timestep is 10 seconds, while the flood module runs at timesteps fluctuate between 5 to 0.5 seconds (depending on the local circumstances). The timestep used for the entire flood domain is the smallest timestep occurring in the flood domain, so the gridcell with the smallest timestep determines the solution.

OpenLISEM is currently in a beta stage concerning this flood module. Both the kinematic wave and the fullswof method have very small mass balance errors, but the coupling of the two methods in OpenLISEM is still under construction. There are two coupling mechanisms:

- It is assumed that the water in the channel cells themselves, instantaneously reaches an equilibrium between the water level in the channel and the flood water level in the strip of land adjacent to the channel. This, therefore, assumes that the channels are not too narrow compared to the cellsize and timestep. This resulting water level is then used to execute the flood module

- It is assumed that runoff water reaching the flood boundary has some momentum and takes some time to mix. Water is turbulent everywhere and the turbulence together with the momentum causes a certain mixing distance. To simulate this additional friction during the mixing a simple assumption has been made: the manning's n of the flooded area is temporarily increased, with a factor depending on the flood depth (in m).

Thus, the kinematic wave for overland flow will change in the flood domain to have a rapid decrease of velocity where the flood water is deeper. These two assumptions about the 1D-2D connection are still under review and being tested.

OpenLISEM presents some disadvantages, as it is a model under development. It simulates flood only from channels, thus missing areas flooded without drainage channels. OpenLISEM considers all overspill from channels to be flood, while in reality this "flood water" may be only a few cm deep. There is therefore some interpretation needed between the direct model output and the phenomenon of the flood as it is perceived by the inhabitants of the area.

Flood simulation with OpenLISEM requires a large number of input maps on rainfall, catchment, land use or land cover, surface properties, infiltration behaviour of the area, channel properties, and house cover with storage capacity (Table 3.2). Some of the input maps have been already available, but other where to be generated. Especially, maps related to catchment, channel properties and infiltration were updated because of the new dataset. A PC Raster script was written for the production all those new maps.

Variable name	Description
Rainfall	
ID	Raingauge zone file
Catchment	
DEM	Digital elevation model (m)
Gradient	Sine of slope gradient in direction of flow ()
LDD	Local surface Drainage Direction network
Outlet	Main catchment outlet corresponding to LDD map
Points	Reporting points for hydrograph
Land use	
Units	Classified land unit map (integers) for output of erosion values
Cover	Fraction surface cover by vegetation and residue (0-1)
LAI	Leaf area index of the plant cover in a gridcell (m2/m2)
Height	Plant height (m)
Road width	Width of impermeable roads (m)
Surface	
RR	Random Roughness (here standard deviation of heights) (cm)
N	Manning's n (-)
Stoniness	Fraction covered by stones (affects only splash det.) (0-1)
Crust	Fraction of gridcell covered with Crust (0-1) (see also Ksat crust)
Compacted	Fraction of gridcell compacted (e.g. wheel tracks)C-)
Hard Surface	No interception/infiltration/detachment (0-1)
Infiltration	
1st layer Green & Ampt	
Ksat l	Saturated Hydraulic Conductivity (mm/h)
Psil	Average suction at the wetting front (cm)
Thetasi	Porosity (-)
Thetail	Initial moisture content (-)
Channels	

Channel properties	
LDD	LDD of main channel (must be 1 branch connected to the outlet)
Width	Channel width (m)
Side angle	Channel side angle (tan angle channel side and surface)
Gradient	Slope gradient of channel bed (-)
N	Manning's n of channel bed (-)
Cohesion	Cohesion of channel bed (kPa)
Channel flood	
Channel Depth	Channel depth, zero (0) depth is considered infinite (m)
Barriers	Flood barriers and obstacles (houses, talus, dikes, in m)
Channel Max Q	Maximum limiting channel discharge. e.g. in culverts (m3/s)
Channel Levee	Height of small channel levee on both sides of the channel (m)
Houses	
House Cover	Fraction of hard roof surface per cell (0-1)
Roof Storage	Size of interception storage of rainwater on roofs (mm)
Drum Store	Size of storage of rainwater drums (m3)

Table 3.2: Input maps for LISEM model

OpenLISEM output

OpenLISEM produces multivariate output information on water and sediments on catchment and subcatchment level. On flood part, OpenLISEM produce tables, maps and time series maps of the total flooded area, flood duration, interception, infiltration, rainfall, slope runoff, drainage discharge, hydrographs that can be used in PC Raster or other spatial analyst or time series software for further analysis. The important evaluated outputs, for this research, were hydrographs to the main outlet, flood extents, flood height, total infiltration (total at), peak time for precipitation P, peak time for discharge Q, peak Q, and the lag time which is the time between the peak time of precipitation and the peak time of discharge.

3.3.2. OpenLISEM simulations

Different flood simulations were run with the aim to analyse the effect of homogeneous (ground records) versus spatio-temporal variable rainfall (WRF rainfall) on flood dynamics characterising Lubigi catchment. In addition, analysis of distribution of rainfall intensities in time was performed on two selected ground recorded rainfalls.

- The first comparison made was between the spatial homogeneous rainfall (25June) and the spatio-temporal variable rainfall (27June WRF simulated).
- The second comparison was between two grounds-measured rainfalls of almost same Ptot but with a different distribution of intensities and duration (25 June and 15Dec).

The Table 3.3 gives the summary of simulations run for this research. In order to be able to compare different simulation some settings were uniformed. The simulation length was set to 2300min, which is the time by which almost all the runoff water not infiltrated reach the main outlet in most of the simulations. The time step was set to 10 seconds and the grid cell size used was 20m to simulate floods a household scale. Hessel (2005) showed that the time step and the grid cell size had an influence on the outputs of OpenLISEM (discharge an soil loss). The units we have chosen were not exactly what Hessel (2005) proposed ,but in a range of the optimum. For all simulations, the rainfall starts with the simulations and total duration of rainfall is equal to the total duration of simulations.

Simulation	Data	Date	Calibration
WRF	WRF	27-Jun	Original
WRF-Ptot			Ptot calibrated
WRF-Imax			Imax calibrated
WRF-homo	WRF used as spatial homogeneous	27-Jun	Original
WRF-Ptot-homo			Ptot calibrated
WRF-Imax-homo			Imax calibrated
OBS-June	Observed	25-Jun	Original
OBS-June-Ksat			0.5*Ksat
OBS-June-Ini			Initial moisture=Porosity
OBS-Dec		15-Dec	Original
OBS-Dec-Ksat			0.5*Ksat
OBS-Dec-Ini			Initial moisture=Porosity

Table 3.3: OpenLISEM simulations made for flood dynamics analysis.

As the modelled rainfall biased from the observed records, the modelled 27June WRF rainfall is compared with the 25June observed rainfall event. In view of different rainfall properties, we calibrated 27June WRF rainfall to match the observed maximum intensity and total precipitation at the grid point of the measurement. In addition, the spatial averages of 27June WRF rainfalls were used in flood simulation, homogenised based on the spatial average. The average rainfall simulated by the WRF model in the catchment was 37.8 mm while Imax was 28mm/h. A multiplication value of 1.75 was used in order to reach a Ptot of 66.2mm measured on the ground while a multiplication factor of 3.75 was used in order to get 106.8mm/h Imax measured on the ground. However, the temporal distribution of WRF rainfall and the measured rainfall was still different which makes comparisons hard. Thus, the spatial average distribution of 27June WRF simulated and its calibrated rainfalls were used as spatial homogenous rainfalls in the fourth, fifth, and sixth simulations.

As a large number of soil samples took by Rossiter (2014) were taken outside the catchment in a completely rural area. This might have led to underestimation of the compaction of soil characterizing urban areas (Gregory et al., 2006; Pitt et al., 2008), see the high hydraulic conductivity (Table 4.1). Gregory et al. (2006) and Pitt et al. (2008) found that even the lowest level of compaction can result in a significantly lower infiltration rate. Thus, all the simulations enforced by observed records were repeated with the Ksat value reduced in half in order to understand the effect of soil compaction on the runoff generation. In addition, the effect of complete non-infiltration was analysed. This research focused on the analysis of one single event, but one single event can be influenced by previous events in the form of moisture content of the soil (Castillo et al., 2003; Zehe et al., 2005).

Finally, as there were no calibration and validation data for simulated flood, for this research the outputs of all 12 simulations were compared to information given by the local population on floods. A comparisons were done using simple linear regression. That's why any flood simulated by OpenLISEM was used for the sake of evaluating the performance in surveyed location. Spatial differences were also identified to test the performance of the model as explained.

4. BASELINE DATA

4.1. Introduction

This chapter focus on the data that were prepared or analysed for input to the OpenLISEM flood analysis. It starts with the results of data collected during the field survey about drainage and the output of the questionnaires. In addition, this chapter gives an overview of soil's hydraulic properties used for this research.

4.2. Soil data for flood simulation

The soil's hydraulic properties are essential for flood simulations (Brath & Montanari, 2000). Rainfall that infiltrates into the soil is usually greater than the part that became runoff, a good estimate of the runoff requires a good estimate of the infiltration (Van Mullem, 1991). OpenLISEM, being the catchment oriented, calculate the infiltration, and depending on the storage capacity of the soil estimate water available for runoff. Thus, accurate soil information leads to accurate runoff estimation. Lubigi catchment soils, used in research, were characterised with high infiltration rate apart from soils found in swamps as can be seen in Table 4.1. According to the report of Rossiter (2014) who investigated the soil's hydraulic properties, particle size classes were dominantly clays, sandy clays and sandy clay loams; silt content was largely low (Figure 4.1: a). The soil parameters were averaged in six landform units shown in Figure 4.1: b. The soil report is influenced by natural soils, with some values taken outside the Kampala city limits. The values should therefore be considered as natural set, vegetated soils with good structure. Compaction effect is less seen the hydraulic conductivity and porosity values Table 4.1.

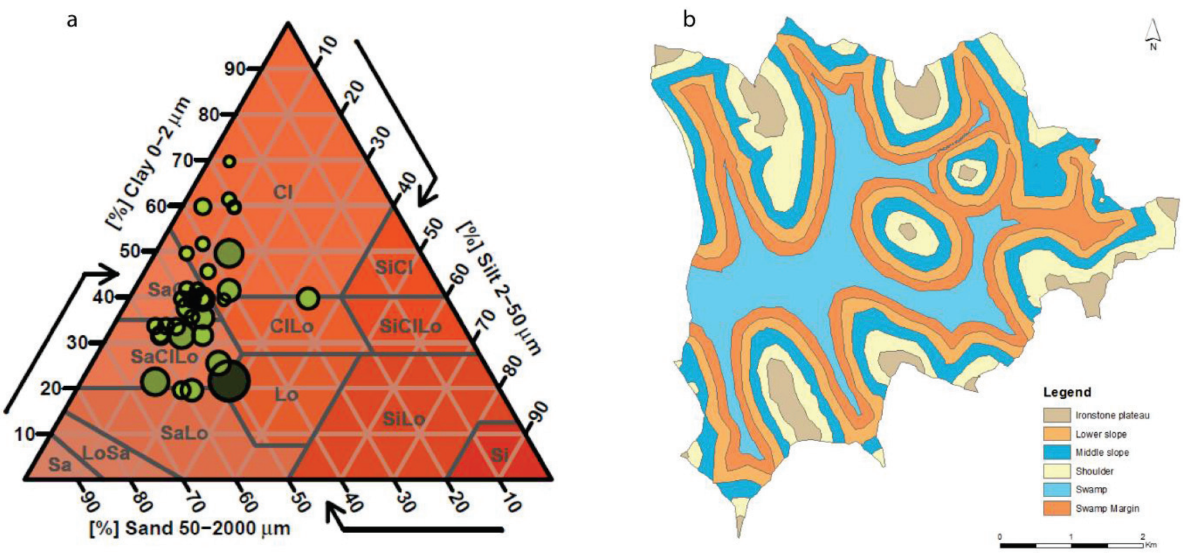

Figure 4.1: a. Soil texture ternary diagram with relative organic matter as post plot. b. is the landform classification .

Landform class	Depth	Ksat	Porosity	Initial soil moisture
Units	mm	mm h-1	proportion	proportion
Ironstone plateau	500	120	0.568	0.5094
Lower slope	1500	75	0.523	0.4707
Swamp	10000	1	0.868	0.7812
swamp margin	2000	50	0.623	0.5607
Midslope	2000	75	0.592	0.5328
Shoulder	1000	120	0.603	0.5094

Table 4.1: Soil's hydraulic properties in Lubigi catchment as used as input in OpenLISEM simulations.

4.3. Drainage channels

Lubigi drainages have been being improved in order to reduce the flooding problems and runoff related issues in general in the past years. Improvements have targeted the increasing size of drainages at it is shown in the Figure 4.2, creation of new channels along roads, improving the construction material by turning the old earth drainages into cements and stones or concrete channels. The Figure 4.3 and Appendix 7.2 give a summary of the measured channel sizes. Primary channels were bigger in size compared to other channels, especially the top and bottom width where the mean of width size is almost three times bigger the size of secondary channels and nearly 8 times tertiary channels. 67% of all drainages are made of cement and stones and 22.5% are made of concrete. Such drainages can influence on the nature of the resulting flood downstream due to the conduction capabilities of such drainages with very low resistance to runoff and flood flow (Arcement et al., 1984).

Figure 4.2: Improvement of the primary drainage channel near the Northern bypass. The primary channel is joined by a secondary channel bringing water from Bwaise.

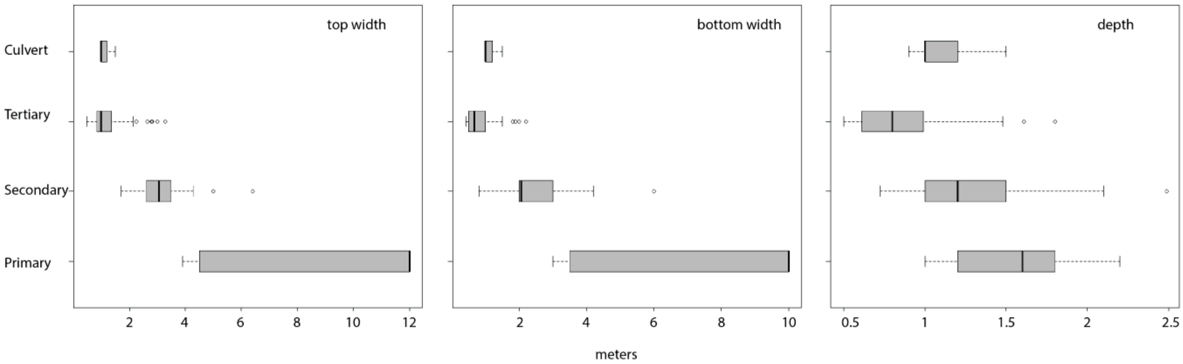

Figure 4.3: Different size characterising drainage channel system in Lubigi catchment, top width, bottom width, and depth.

There is not much difference in the depth of drainages. 75% of secondary channels have a depth below 1m. Both primary and secondary are mostly deeper than one meter. Culverts are seen as one of the causes of floods according to respondents. Also highlighted by Tingsanchali (2012), a major cause of local flooding was the drainage facilities blocked with garbage. Culverts, numerous due to road networks, are with small size as shown in Figure 4.4 and can easily be filled with solid wastes. The problem related to solid waste the city is facing as shown by Matagi (2002) and Oyoo et.al (2013). Beside solid waste, the status of some drainages is precarious as they are every time sedimented during rainfall or eroded as seen in Figure 4.4 c and d thus increasing the flood risk according to local authority of KCCA. Not all the drainages measured where used in flood simulation as some were very narrow mainly tertiary channels. Figure 4.5 shows in details the input channel sizes used in flood simulations in terms of depth and width.

Figure 4.4: Culverts are filled with garbage in (a) and (b). (c) shows KCCA employee removing sediments filling a channel in Bwaise while (d) show a damaged secondary channel.

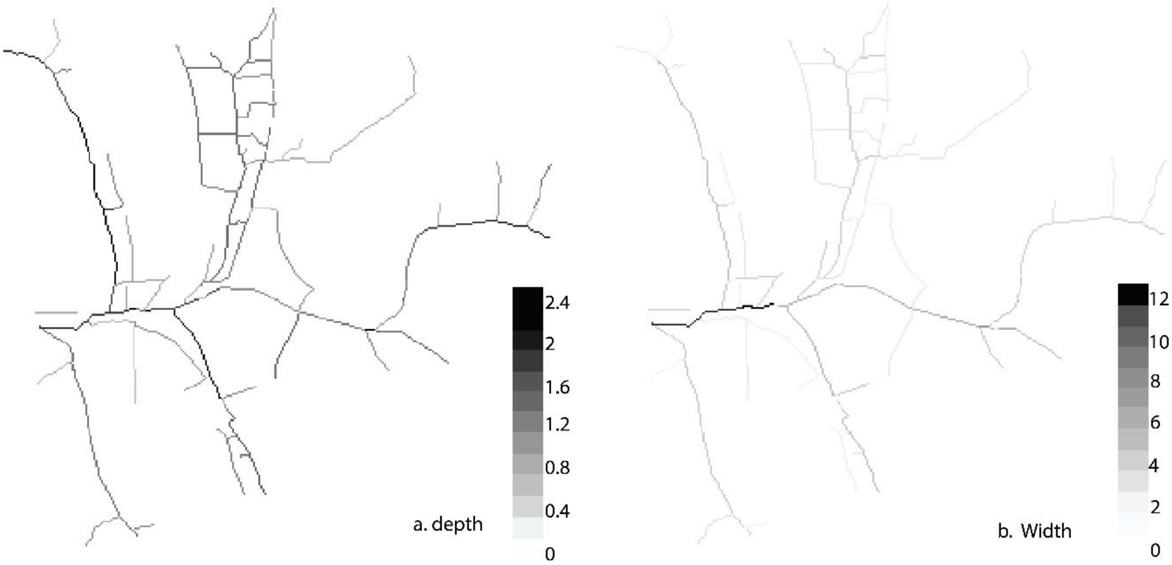

Figure 4.5: Channel depth (m) and with maps (m) used as input in flood simulation.

4.4. Flood survey

Getting accurate information from the population living on Lubigi catchment's marginal land is a challenging issue due to the problem of land access and informal ownership the city is facing (Nkurunziza, 2008). However, from physical evidences one can tell how vulnerable the residents of Lubigi lowlands ares. From abandoned houses (Figure 4.6), different coping mechanism (Figure 4.7), local population adapts to floods or lose their lands. As shown in Figure 3.3: a., most of respondents live in a former wetland which is very flat (gradient less than 0.2%) not allowing fast movement of water (Figure 2.2).

Flood occurrence	Household	Percent	Valid Percent
1	9	6.8	8.9
2	16	12	15.8
3	9	6.8	8.9
4	4	3	4
5	1	0.8	1
Rain season	35	26.3	34.7
When heavy	27	20.3	26.7
Total	101	75.9	100
Not flooded area	32	24.1	
Total	133	100	

Table 4.2: flood recurrence times per year according to respondents

Figure 4.6: Abandoned houses because of floods. b and c are seen to be below the level of other surrounding grounds which is due probably to a sinking process or neighbours who elevated houses leaving others in a hole.

Figure 4.7: Different flood coping strategies. Water trapped inside the house because of the protection put around the house (second image from the left).

Among respondents, 75% have been living in the area for more than three years and another 25% live in the area for 1 or 2 years. Respondents show to have a vague idea about the recurrence of flood per year. 26.3% of the respondents said to experience floods during the rainy season while and 20.3% when the rain is very heavy (Table 4.2). Depending on the time spend in the area, respondents who have been living in the area for longer period said to be unaware of flood problem by the time they settled in the catchment compared to those who recently moved in the area (Figure 4.8). Probably, the flood problem increased in time with the urbanization process as highlighted (Douglas et al., 2008).

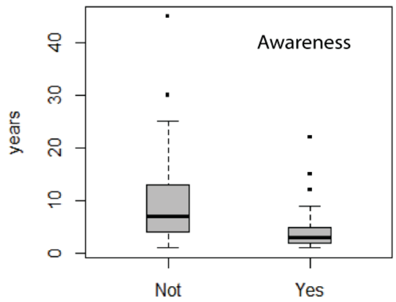

Figure 4.8: Flood awareness before coming to settle in Lubigi floodplains in relation to time spend in the floodplain

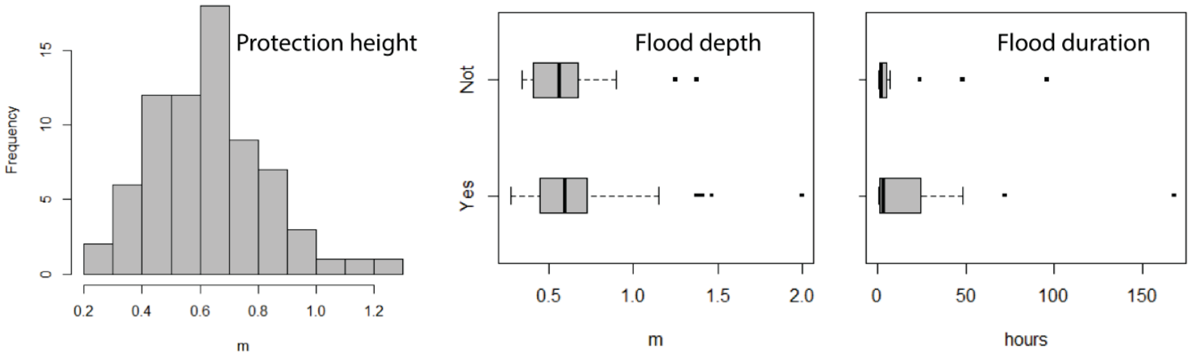

Figure 4.9: The histogram shows the distribution of measured protection against flood, while the two boxplot shows flood depth and duration depending on being protected or not.

One sign of change in behaviour of people exposed to flood risk is that they try to adapt by protecting themselves against the flood (Tapsell et al., 2002). Figure 4.7 shows examples of protection mechanism adopted by the population living in Lubigi floodplains. Mainly, they protect houses against flood water to enter inside the house though protections do not guarantee safety. The protection height reflect how severe are flooding in a given location. Some build a protection around the door or small dyke around the whole house while other elevates the ground level before construction. Respondent without protection reported longer hours of flooding when compared to respondent with protection, while they seem to suffer same flood depth as it is shown in Figure 4.9. This concurs with the statement of Jha et al. (2012) that lack of flood defence mechanisms can increase the vulnerability. Unprotected houses experience longer periods of flooding. As shown in Figure 4.11, people whose water enter the house reported to suffer longer hours and deeper flood compared to those whose water do not enter inside the house. This can be seen as an example of what Kundzewicz (1999) highlighted that there is a difference to flood vulnerability between even neighbouring households which can be enormous especially in less developed countries.

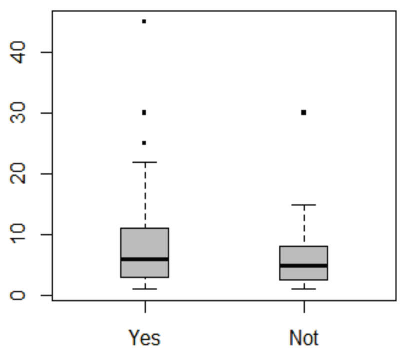

Figure 4.10: Households protecting their houses depending on the time spent in the area

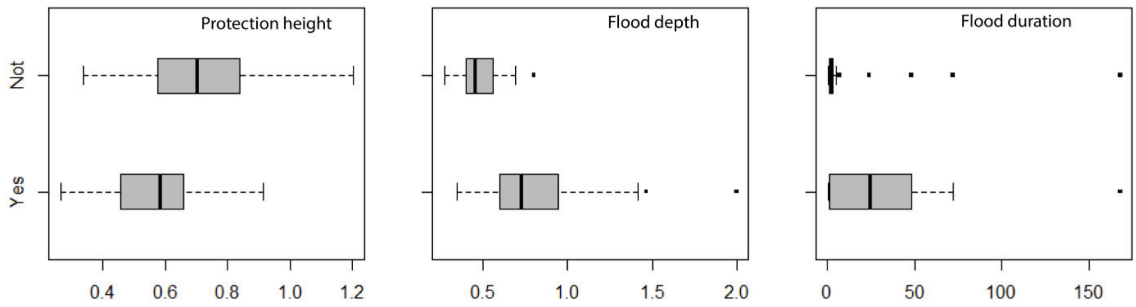

Figure 4.11: Depending on whether water enters in the house or not, this figure shows the measured protection height (m), the depth (m) and of flood (h).

4.5. Rainfall for flood simulation

4.5.1. Ground record

Only rainfall recorded at Makerere university station were used. Simply, Rainfall recorded at Outspan primary school presented some gaps and bigger time steps (1hour).Following the criteria discussed in section 3.2.1, 77 rainfall events have been identified from the period between the 14th of May 2012 up to 11th of May 2013 with 1027.99 mm of rainfall depth for almost a complete year. This amount is very low compared to an annual average between 1200-2000 mm per year characterising the area highlighted by Matagi (2002) and NEMA (2009). This mismatch can be explained by the fact that some of the rainfall events recorded were ignored as they did meet the criteria fixed for a single primitive rainfall during this research.

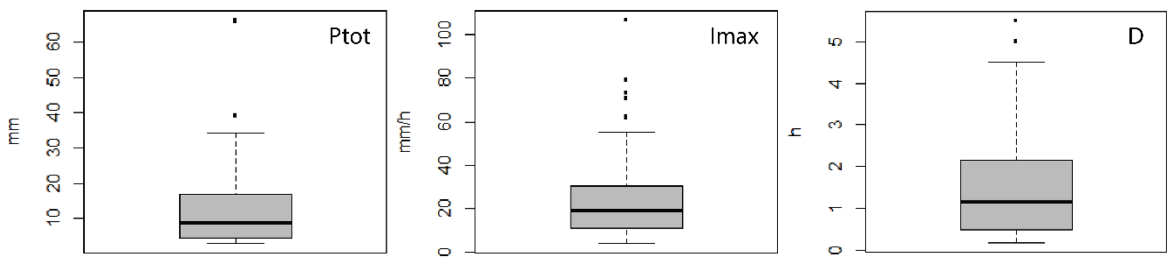

Figure 4.12: Distribution of three main characteristics of rainfall events of Lubigi catchment. Ptot is mm, Imax in mm/h , and D is in hours.

The longest rainfall recorded was 5h5 hours for a rainfall event that occurred the 15th of December 2012. 75% of rainfalls in the catchment are below 2h10' (Figure 4.12). Furthermore, Figure 4.12 shows that the highest rainfall depth was 66.2mm, which is a rainfall event that occurred the 25th of June 2012, while 16.8mm is the 75th percentile. The highest intensity measured was 106.8 mm/h and 75% are below 30.4 mm/h (Figure 4.12). According to the research done by ACE (2010), a 61mm rainfall event is said to be a two year return rainfall. Note that in this research two rainfalls one of 66.2mm, and one of 65.8mm were identified in the year of 2012 when rainfall event is defined from Brown et al. (1985), contrary to the daily basis used by ACE (2010).

The comparison between afternoon and morning rainfall showed that the rainfall events in the mornings have longer durations and receives more Ptot than the afternoons, while they overlap for Imax (Figure 4.13). All rainfalls that occurred in the afternoons were with a duration below 3 hours while for rainfalls that occurred in the afternoon almost 50% where with a duration above 3 hours. However, the afternoons counted more rainfall events compared to the mornings, 45 against 32. This afternoon precipitations are probably related to convection characterizing areas surrounding Lake Victoria as highlighted by Maidment et al. (2013).There was a strong correlation between Imax and Ptot compared to the correlation between D and Ptot as can be seen in Figure 4.14. However, the correlation between D and Imax is very low. The Spearman's r between Ptot and Imax is 0.79, 0.61 between Ptot and D, while it is only 0.21 between Imax and D. This concurs with what Matagi (2002) also showed that rainfall over in Kampala is mostly short in duration but with high intensity causing floods often as said also respondents. Still, longer time records are necessary in order to come to a concrete conclusion. But, one can say that most rainfall events with longer duration are caused probably by ITCZ while shorter in duration are convectional rainfall locally generated with reference to findings of Ba and Nicholson (1998) who analysed the convection activities around Lake Victoria.

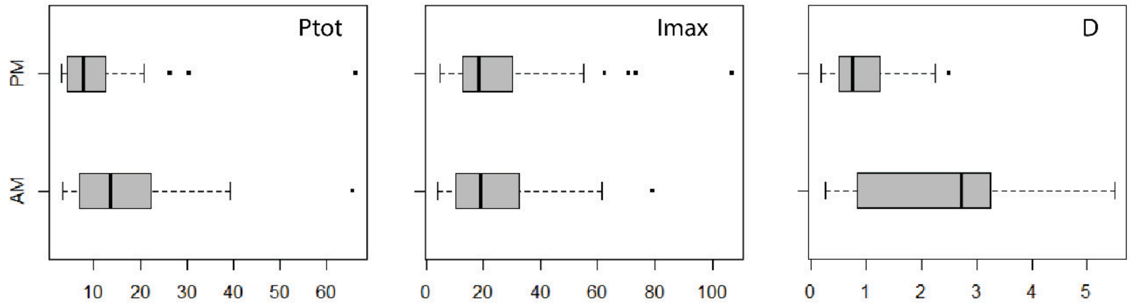

Figure 4.13: Comparison between mornings and afternoons rainfall events. Ptot is mm, Imax in mm/h , and D is in hours.

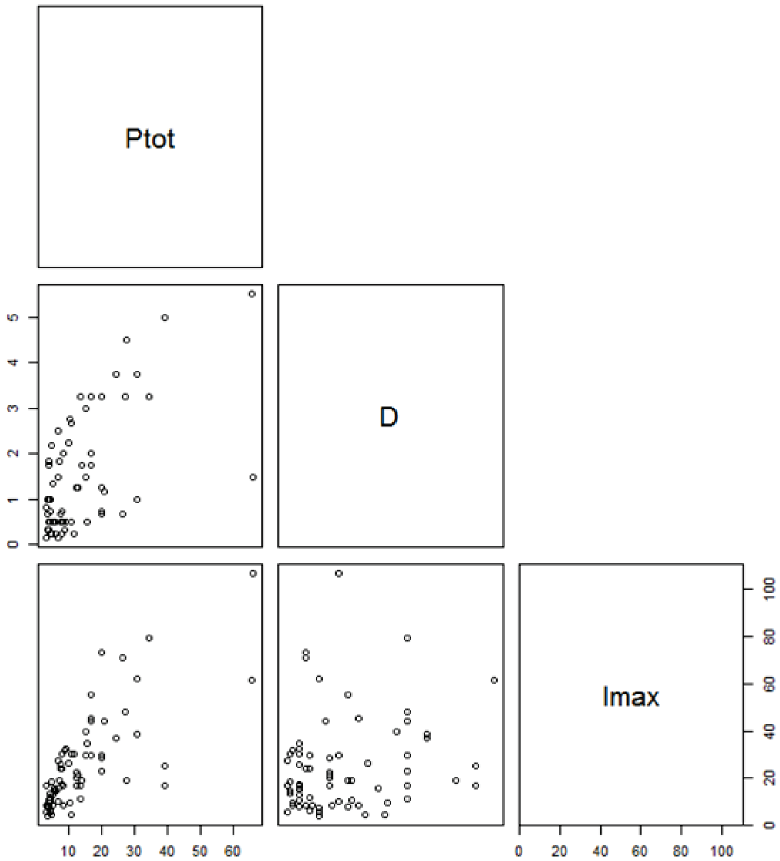

Figure 4.14: Correlation between different characteristics of rainfall events. Ptot is mm, Imax in mm/h, and D is in hours.

4.5.2. WRF model rainfall

Dr. Ettema/ITC simulated the atmospheric conditions for a 6days period, starting 23June 2012, around the rainfall event of the 25th of 29June 2012 using WRF model (Skamarock et al., 2008). The model was with less moisture or dry to give rainfall similar to the observed rainfall the 25June. The model simulates the atmospheric conditions that lead to rainfall, and needs a correct initialisation. It is therefore not easy to simulate exactly the circumstances that lead to the 25th June 2012 event. In addition, the model is known to cause rainfall when the atmosphere has lower moisture contents than in reality, so that the simulated rainfall is often early and less intense compared to ground measurements (Pennelly et al., 2014).

A major rainfall event started the 27th of June 2012 at 09:40 AM. Rainfall simulated by WRF model was highly variable as can be seen in Figure 4.16 and Figure 4.17. Most of the variogram were with high nugget probably related to high rainfall variability in a single time step itself (Bivand et al., 2013). In addition, the high spatial variability of rainfall can be expressed by a wide range of variogram models used. In general, WRF model simulated high intensities especially in the northern part of Kampala or northeast of Lubigi catchment (Figure 4.17 a&b). The highest simulated Ptot was 90.9mm over Kampala and 90.3mm over Lubigi while the lowest was 0 and 7.2mm respectively (Figure 4.17:b). As shown in Figure 4.17, the highest rainfall intensities were located in the north where it reached 96mm/h.

The spatial average of the rainfall simulated by the WRF model over Kampala and Lubigi catchment was 37.8mm of Ptot, meaning 57.19% of the observed rainfall. The highest Imax average was 28mm/h inside the catchment with total D of 3 hours. According to WRF simulation, Makerere station received around 19mm of precipitation, meaning only 30.54% of rainfall recorded by ground station. It is important to mention that the month of June mark the end of rainy season and the start of a dry season in the southern part of Uganda where Kampala is located (Maidment et al., 2013). The whole month of June have received 101.6mm of rainfall in 3 rainfall events; the 14th (26.4mm), 25th (66.2mm), and 30th (9mm) according to ground records. In the case of Kampala, one can say that WRF model could not capture the local processes of rainfall generation characterising the area, but also the fact that warm season rainfall simulation is very challenging as said Gallus and Bresch (2006).

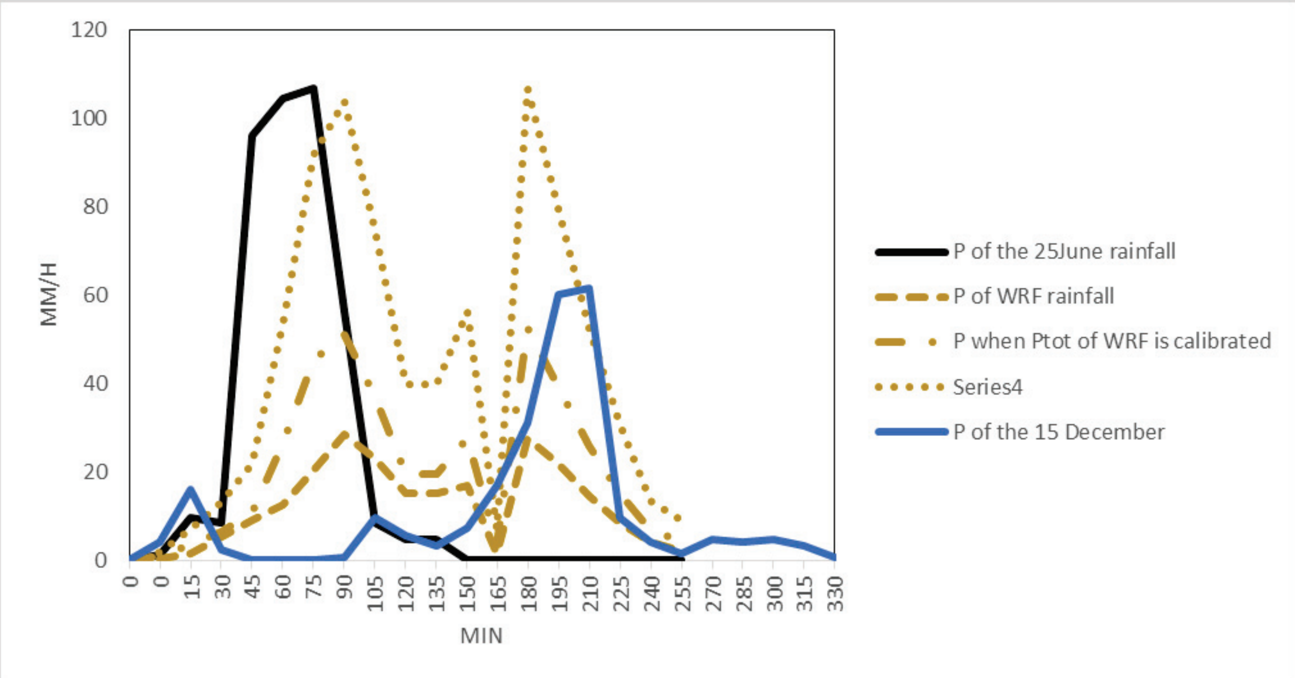

Figure 4.15: The temporal distribution of intensities of ground measured rainfall and the rainfall simulated by WRF model. Including the distribution of intensities when WRF model rainfall in calibrated to meet the ground measurement on Imax and Ptot.

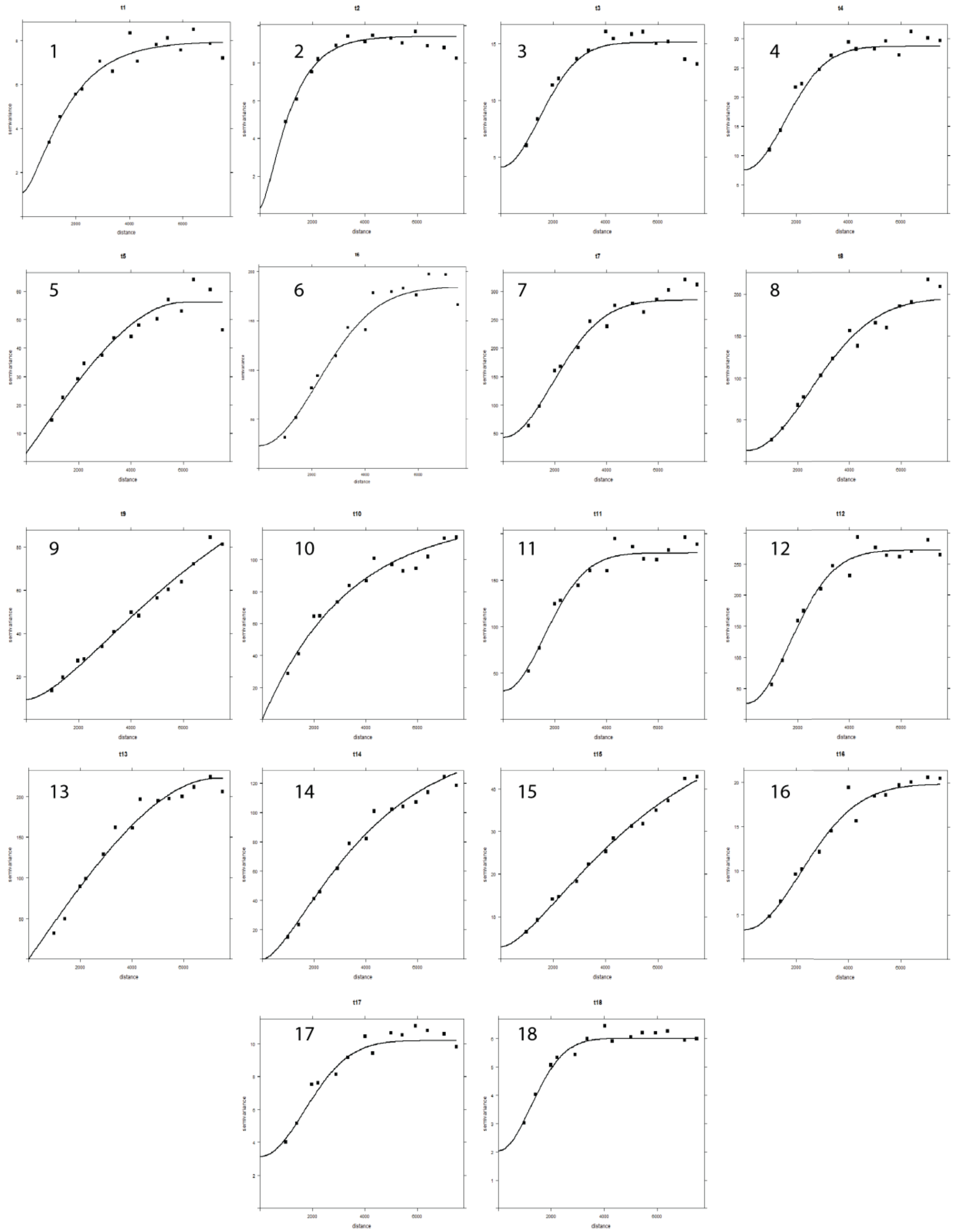

Figure 4.16: Variogram models of the 27June WRF rainfall starting at 09:40 AM with 10min step. Every variogram was fitted with different variogram model; a Bessel model was used for time steps 1, 2, 9, 14, 15. A Gaussian model was used for time steps 3, 4, 6, 7, 8, 11, 12, 16, 17, and 18. A Spherical model was used for time step 5, and 13 while the exponential model was only used for 10th time step. The model choice was based on the best fit.

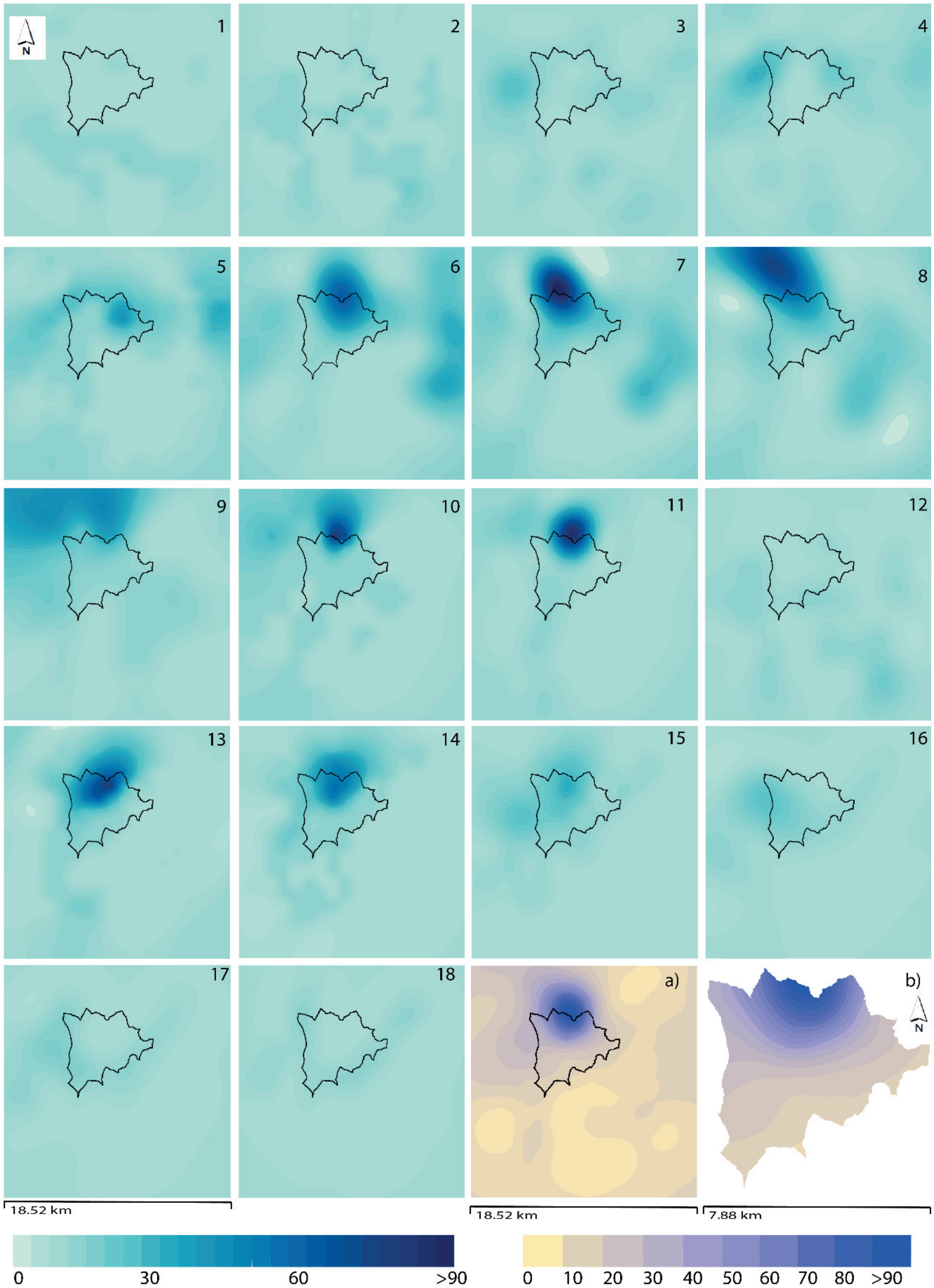

Figure 4.17: 1-18distribution of rainfall intensities of the 27June WRF rainfall starting at 09:40 AM with 10min step over Kampala. The black outline shows Lubigi catchment. a: 27June WRF rainfall ‘s Ptot distribution over Kampala. B: 27June WRF rainfall‘s Ptot distribution over Lubigi catchment.

5. OPENLISEM ANALYSIS

5.1. Introduction

This chapter focuses on the Lubigi flood dynamics analysis using OpenLISEM with different rainfall data. It explores how different simulations (Table 3.3) are compared in terms of infiltration, peak time, peak discharge, hydrographs, flood depth, flood duration, flood extent, and total discharge. The comparison was done between homogeneous and spatio-temporal variable rainfalls. Furthermore, this chapter compared observed homogeneous rainfalls with different intensity distribution in time. Table 5.1 gives a summary of the results from all twelve simulations run. Finally, the results of simulations were compared to the perception of the population on floods they experienced in their neighbourhood in terms of depth and duration.

5.2. Impact of spatial variability of rainfall on flood dynamics

OpenLISEM simulations using spatial variability of rainfall led to different hydrological response on the catchment level compared to homogeneous rainfall. As can be seen from the infiltration, flood depth and flood duration (resp. Figure 5.1, Figure 5.2, and Figure 5.3), simulations using spatio-temporal variable 27June WRF rainfall show more hydrological activities on the northern side of the catchment. There was a huge difference between the WRF's spatial average and the highest simulated Ptot and Imax (Figure 4.17, Appendix 7.3, and Appendix 7.4), this resulted in clear spatial differences in hydrolodical processes when WRF rainfall was used in flood simulations. In general, simulations using spatio-temporal rainfall led to more floods in the northern part compared to when spatial homogeneous rainfall is used. Which is simply a result of more rainfall activity in that part. The results of simulations using homogeneous rainfall have shown homogeneous rainfall infiltration in same land units, and depending on water available for runoff, hydrological response are distributed equally inside the catchment. Hydrographs of simulations using homogeneous rainfall (black lines in Figure 5.4 and Figure 5.5) have all higher peaks and very steep hydrograph compared to when spatio-temporal variable rainfalls are used. When homogeneous rainfall is used, the entire area responds at the same time and all water from the side valleys accumulates in the central valley roughly at the same moment. This causes a lot more discharge. However, when spatio-temporal rainfall is used the falling water level had longer duration as can be seen in all hydrographs (Figure 5.4 and Figure 5.5). This is mainly due to fact that the areas receiving higher rainfall when WRF model is used are located far from the main outlet.

5.2.1. Spatio-temporal WRF rainfall versus homogeneous observed rainfall impacts

Simulations in this section used 27June WRF rainfall and the observed 25June rainfall (OBS-June). The comparison between the results of both simulations was very challenging as both had different rainfall input characteristics in terms of Ptot, Imax, D, peak time for P and even peak time for Q (Figure 4.15, and Table 5.1). The infiltration rate was high on both WRF and OBS-June simulations, leaving less water available for runoff, 3.9 and 11.9mm respectively in total discharge. The WRF had the lowest values in terms of total infiltration, discharge, flood volume and the flooded area. However, the difference in flood depth was not significant. The highest flood depth in the catchment was 1.62 m for WRF while it was 1.82m for OBS-June. The OBS-June showed wider flood extent (Figure 5.2) and more areas that stayed flooded for longer periods (Figure 5.3).

	WRF	WRF-Ptot	WRF-Imax	WRF-homo	WRF-Ptot-homo	WRF-Imax-homo	OBS-June	OBS-June-Ksat	OBS-June-Ini	OBS-Dec	OBS-Dec-Ksat	OBS-Dec-Ini
Simulation time (min)	2299.7											
Area (m2)	28160000											
Ptot (mm)	37.9	66.2	134.2	37.9	66.2	134.2	66.2	66.2	66.2	65.6	65.6	65.6
Total Q (mm)	3.9	15.7	51.9	3.2	7.9	53.6	11.9	22.8	66.2	10.5	11.4	65.3
Total inf (mm)	33.1	49	68.5	34	56.6	78	52.1	42.1	0	57.2	52.2	0
Total Q (m^3)	108133	436706	1411375	78629	204056	1428463	316944	618440	1778513	286623	308697	1753369
Peak Q (l/s)	6049.1	12488.5	23823	8075.9	12517.7	31246.2	24796.6	28140.7	38559.4	16262.7	21416.6	30785.5
Peak time P (min)	60.2	120.2	120.2	50.5	110.5	110.2	50.2	50.2	50.2	210.2	210.2	210.2
Peak time Q (min)	175.2	171.3	179	151.8	141.8	158	77.2	96	91.2	235.2	241.3	250.3
Q/Ptot (%)	10.3	23.7	38.7	8.4	12	40.1	18	34.5	99.7	16	17.4	99.6
Flood volume (m^3)	81698.3	432640	2005287	25461	138270	1357747	285811	644551	1964969	158827	266754	1598860
Flood area (m^2)	265600	854400	2068800	124000	395600	2257600	913200	1670000	2796400	500000	814800	2408000

Table 5.1: Results of all 12 OpenLISEM flood simulations (Table 3.3) using the rainfall. Simulation from s1 to s6 uses 27June WRF rainfall and its derivative (homo=homogeneous), s7 to s9 are the results of simulation the 25June rainfall. s10 to s12 results of the simulation using 15December rainfall.

5.2.2. Calibrated modelled rainfall impacts

The calibration of WRF's spatial average of Ptot gave a Ptot value similar to the 25June observed rainfall (Table 5.1and Appendix 7.4). Yet, the calibrated spatial precipitation pattern shows very high rainfall in the northern part where Ptot reaches 194mm and Imax of 168.5mm/h. The higher Ptot is almost equal to the 200 year return as shown in from the research done by ACE (2010). The simulation results in Table 5.1 show that the WRF-Ptot had much water in the discharge when compared to OBS-June, 15.7 and 11.9mm respectively. The peak discharge of WRF-Ptot was lower but the total discharge and the flood volume were higher compared to the OBS-June. However, when it comes to the flooded area, the OBS-June had wider flooded area (Figure 5.2). This contradiction can be explained by the fact that 27June WRF rainfall was less in the southern part of Lubigi, thus restricting intense hydraulogic activities only in the northern part of the catchment. The northern part of the catchment stayed flooded for longer period in the WRF-Ptot (Figure 5.3). The deepest flood depth was 2.5m for the WRF-Ptot against 1.8m of the OBS-June.

The calibration of WRF model's Imax gave a value of Imax closer to the observed (106.8mm/h). However, the spatio-temporal average of Ptot (134.2mm) was more than the double of the observed (66.2mm). The highest Ptot was 392.8mm and Imax of 361.3mm/h in the north, which is seen as unrealistic for an event of 3hours in relation to the report made by ACE (2010). With 51, 9mm of rainfall available for runoff against 11.9mm, the results of the WRF-Imax were very high compared to the results of the OBS-June (Table 5.1). In Figure 5.4, WRF-Imax shows two peaks and falling water level of longer duration. However, the OBS-June kept the higher peak discharge. The southwest of the catchment is still without floods for WRF-Imax (Figure 5.2 and Figure 5.3). Some areas in the northern part of the catchment shown the flood depth of 11.6m in WRF-Imax, this unrealistically high and might be due to a simulation error. As can be seen in Figure 5.2 and Figure 5.3, the northern part in WRF-Imax was disconnected to the general water cilcuration. This same error explains why the sum of total infiltration and total discharge were showing a huge mass unbalance in comparison to the Ptot. Note that, the Table 5.1 does not show all the sinks. When the total is less than 100%, it means that there is still isolated flood water at the surface or held in interception (house and vegetation).

5.2.3. Spatio-temporal WFR versus homogeneous WRF impact

Simulations in this section used 27June WRF rainfall either as either spatio-temporal variable rainfall or as spatial homogeneous in flood simulation. The results of simulation are summarized in Table 5.1. WRF and WRF-Ptot simulations had more water available for runoff WRF-homo and WRF-Ptot-homo simulation. The total infiltration was lower in simulations using spatio-temporal variable rainfall compared to simulations using homogeneous rainfalls. The exception is WRF-Imax and WRF-Imax-homo, probably due to the error explain in section 5.2.1. The spatio-temporal variable rainfall based simulations had more water for runoff, thus higher flood volume, total discharge, and wider flooded area except WRF-Imax versus WRF-Imax-homo. Note that in Figure 5.1, Figure 5.2, and Figure 5.3, hydrological processes are intense in the northern part of the catchment spatio-temporal variable rainfall is used. The hydrographs in Figure 5.5 shows that spatio-temporal rainfall based simulation had longer falling limb compared to spatial homogeneous, while the spatial homogeneous based simulation kept the higher peak discharge. In addition, the WRF-Imax shown two peaks while the WRF-Imax-homo did not. This concurs with the findings of P. Arnaud et al. (2002) that spatio-temporal rainfall influence not only the runoff but, also the peak discharge and time shift of hydrographs.

5.3. Rainfall properties impact

The simulations in this section used two observed rainfall of almost same Ptot but with a different distribution of Imax and D, 25June and 15June rainfalls. The results are summarized in the Table 5.1. The simulations shown that, both contributed almost same amount of rainfall to total discharge. The OBS-June had higher peak discharge, flood volume and wider flooded area. This is mainly due to faster time to peak and higher rainfall intensities compared to OBS-Dec. The shorter time between precipitation onset followed by higher runoff peaks have been shown to result into higher discharges (Shuster et al., 2005) because of fast flow excess (Haga et al., 2005). Note that the overall infiltration was slightly higher for the

OBS-Dec (Figure 5.1) mainly due to a negative correlation between rainfall intensity and positive correlation with duration of rainfall on soil infiltration (Hawke et al., 2006; Y. Li et al., 2006). The OBS-June resulted into deeper floods and of longer duration compared to the OBS-Dec (Figure 5.2 and Figure 5.3). Note that the OBS-Dec had a mass balance error, which is probably also linked the long hydrograph of longer duration in Figure 5.6. When the total is more than a 100%, this is a true model error. OpenLISEM does not do a real iteration. An iteration is an algorithm that calculates the flood level again for a timestep, if the mass balance is not correct. The next iteration step has then a smaller timestep so that the changes for error are smaller. Lisem uses the fullSWOF2D method, which uses a best guess for a small timestep, and then, according to the mass balance error it calculates the next step with a smaller or bigger timestep. The timestep is adapted according to what happened in the previous timestep. This may lead to errors when there is really a lot of sudden changes (Delestre et al., 2009).

5.4. Initial soil conditions and soil's properties impacts

The impacts of initial soil conditions were analysed using the 25June and 15December rainfalls. The results of four OpenLISEM flood simulation (OBS-June-Ksat, OBS-June-Ini, OBS-Dec-Ksat, and OBS-Dec-Ini) are compared in relation to the results of OBS-June and OBS-Dec (Table 5.1). The reduction of Ksat by half resulted in a double increase of water available for runoff in the OBS-June-Ksat (11.9mm in OBS-June to 22.8mm) while it increased only by 0.9mm in the OBS-Dec-Ksat (from 10.5mm in OBS-Dec to 11.4). There was an increase on both sides in terms of peak discharge, flood volume, flooded area, but the increase was very high for OBS-June. Which concurs with what was said above in the section 5.3 on the role intensity distribution, and duration on the resulting runoff dynamics and floods. The simulations using the 25June rainfall had all higher and steeper hydrograph related to higher intensities of the rainfall (Figure 5.6).

When the initial moisture was made equal to the porosity in order to saturate the soil at the beginning, one should notice in the Table 5.1 that both rainfalls produced almost the same amount of total discharges. On the other hand, flood simulation using the 25th June rainfall (OBS-June-Ini) had higher peak discharge, total discharge, flood volume and wider flooded area. The distribution of rainfall intensities and duration was judged essential, but also the initial conditions are highly needed especially when analysing rainfalls of higher intensities in Lubigi catchment. Higher hydraulic conductivity of soils shown in Table 3.2 leaves less water for runoff, especially when intensities are low. However, as the catchment longer rain seasons, the better knowledge initial moisture content can lead to better flood estimation. Seen the high infiltration rate characterizing Lubigi catchment, floods are probably linked to rainfall of high intensities (Matagi, 2002) or simply the hydraulic state of soils (Gregory et al., 2006; Pitt et al., 2008).

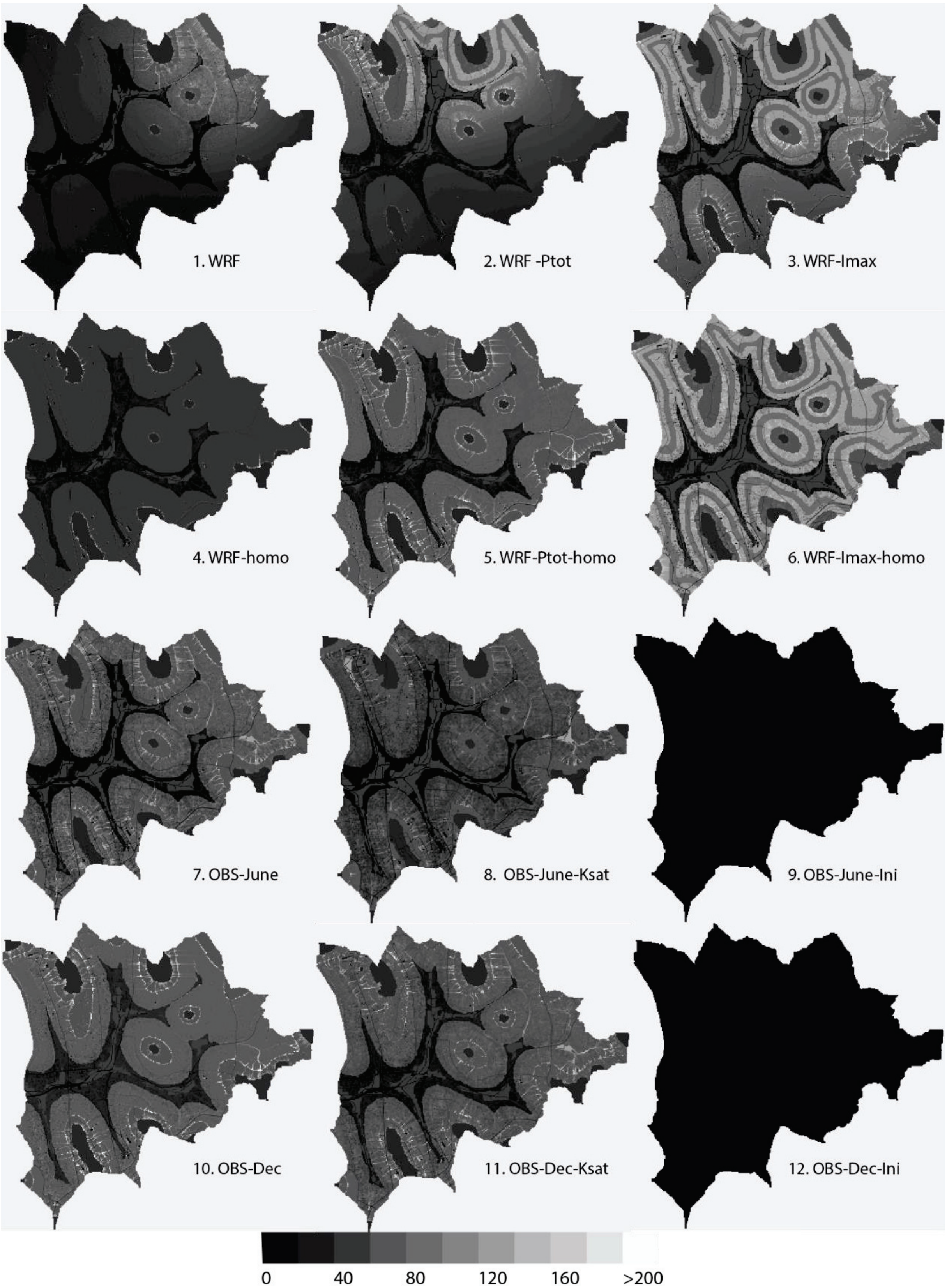

Figure 5.1. Infiltration maps in mm of all 12 OpenLISEM flood simulations (Table 3.3) using the rainfall. Simulation from 1 to 6 uses 27June WRF rainfall and it’s derivative, 7 to 9 are the results of simulation the 25June rainfall. 10 to 12 results of the simulation using 15December rainfall.

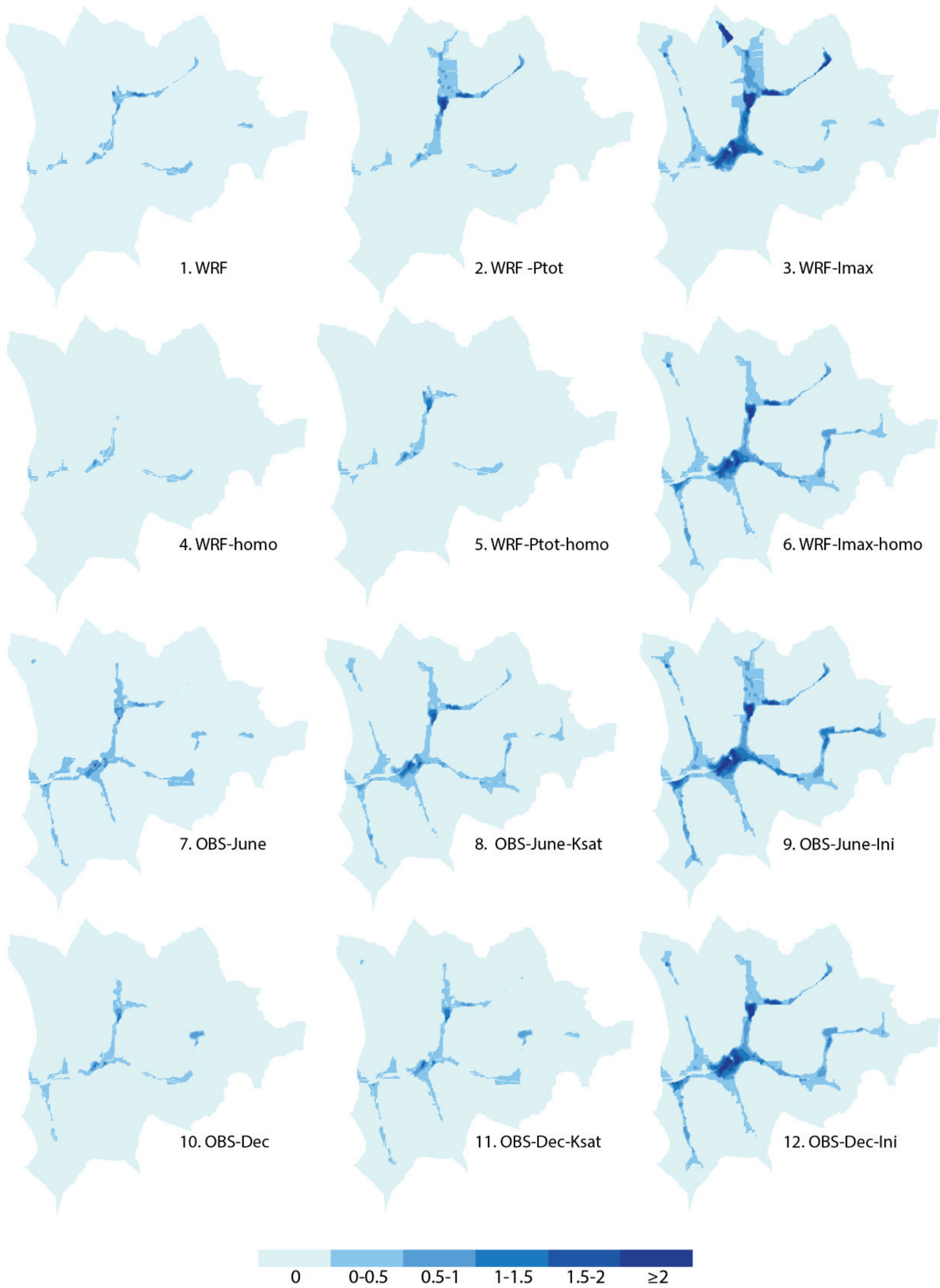

Figure 5.2: Flood depth maps in m of all 12 OpenLISEM flood simulations (Table 3.3) using the rainfall. Simulation from 1 to 6 uses 27June WRF rainfall and its derivative, 7 to 9 are the results of simulation the 25June rainfall. 10 to 12 results of the simulation using 15December rainfall.

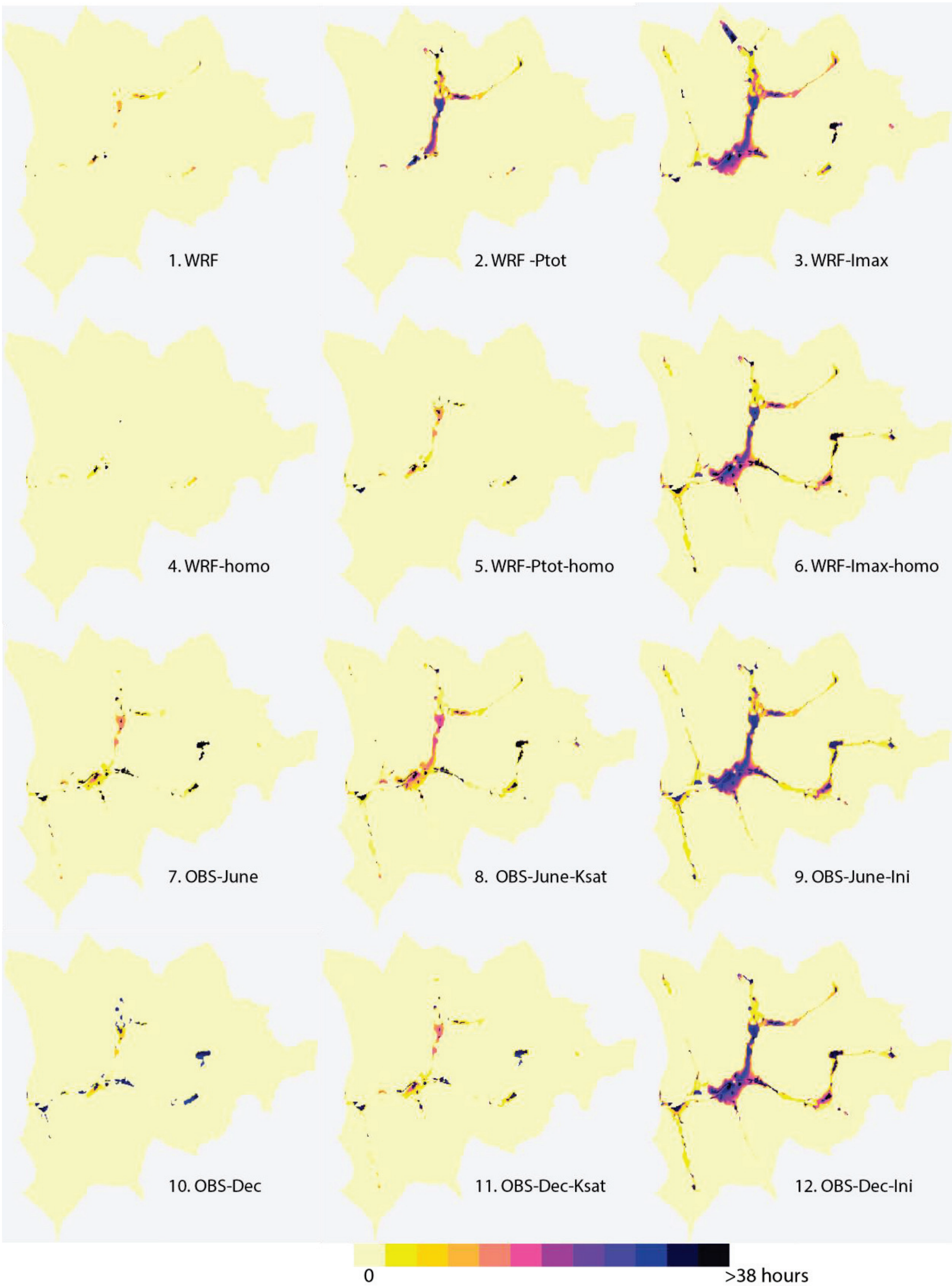

Figure 5.3: Flood duration maps in hours of all 12 OpenLISEM flood simulations (Table 3.3) using the rainfall spatio-temporal rainfall and homogeneous rainfall. Simulation from 1 to 6 uses 27June WRF rainfall and its derivative, 7 to 9 are the results of simulation the observed 25June rainfall. 10 to 12 results of the simulation using observed 15December rainfall.

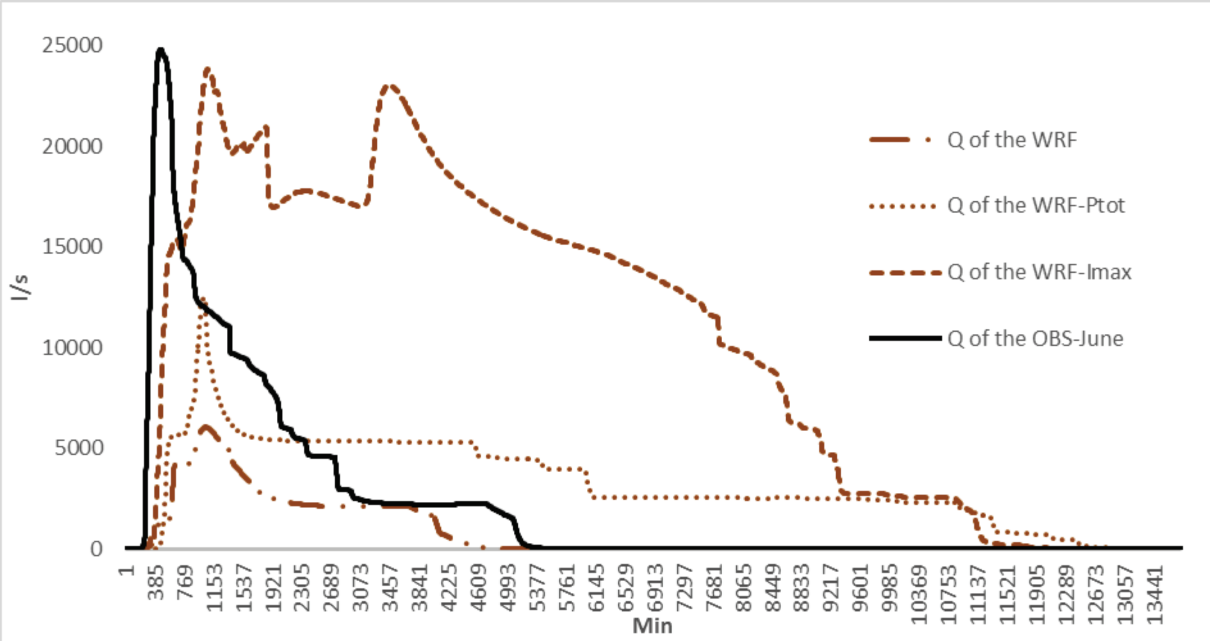

Figure 5.4: Discharge hydrograph at the main outlet of the four OpenLISEM simulations using WRF rainfall and when WRF is calibrated and with the observed rainfall of the 25th of June 2012 (WRF, WRF-Ptot, WRF-Imax and OBS-June).

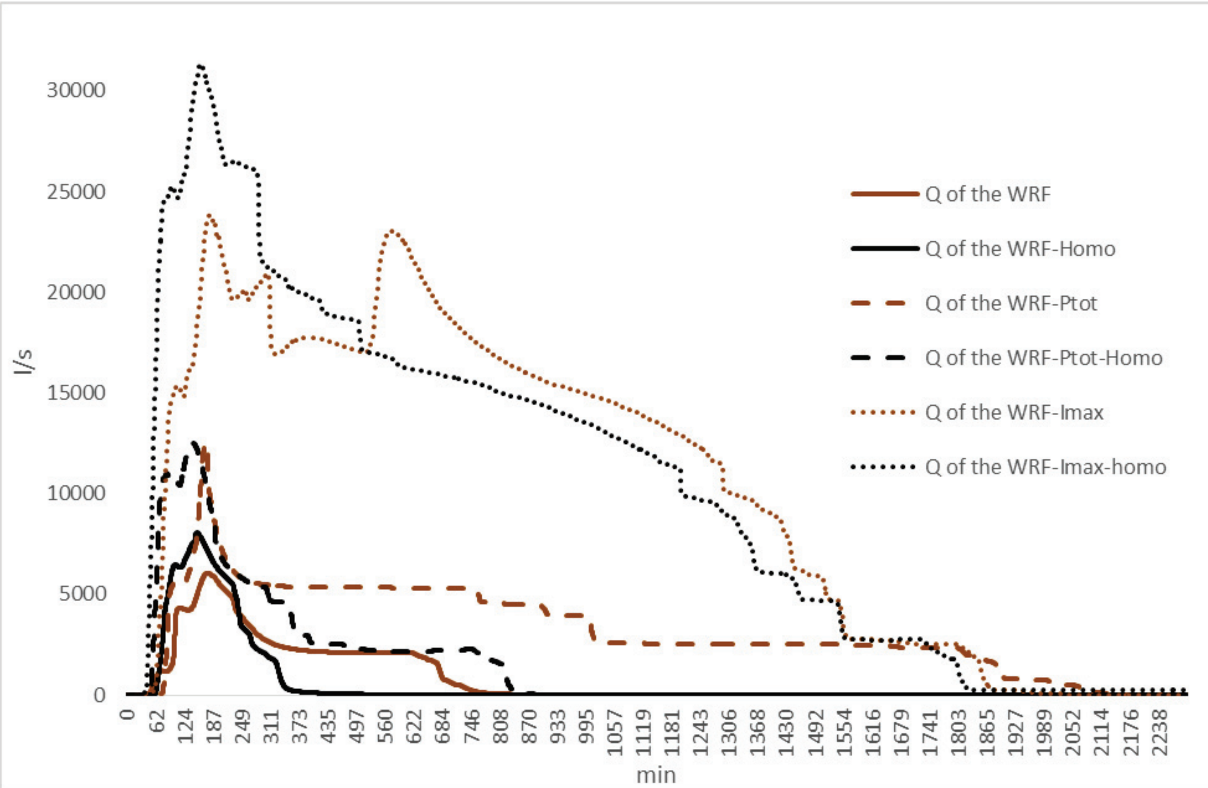

Figure 5.5: Discharge hydrograph at the main outlet showing WRF rainfall and when it is calibrated on Ptot and Imax with the comparison of when WRF rainfall derivatives used as spatial homogeneous rainfalls.

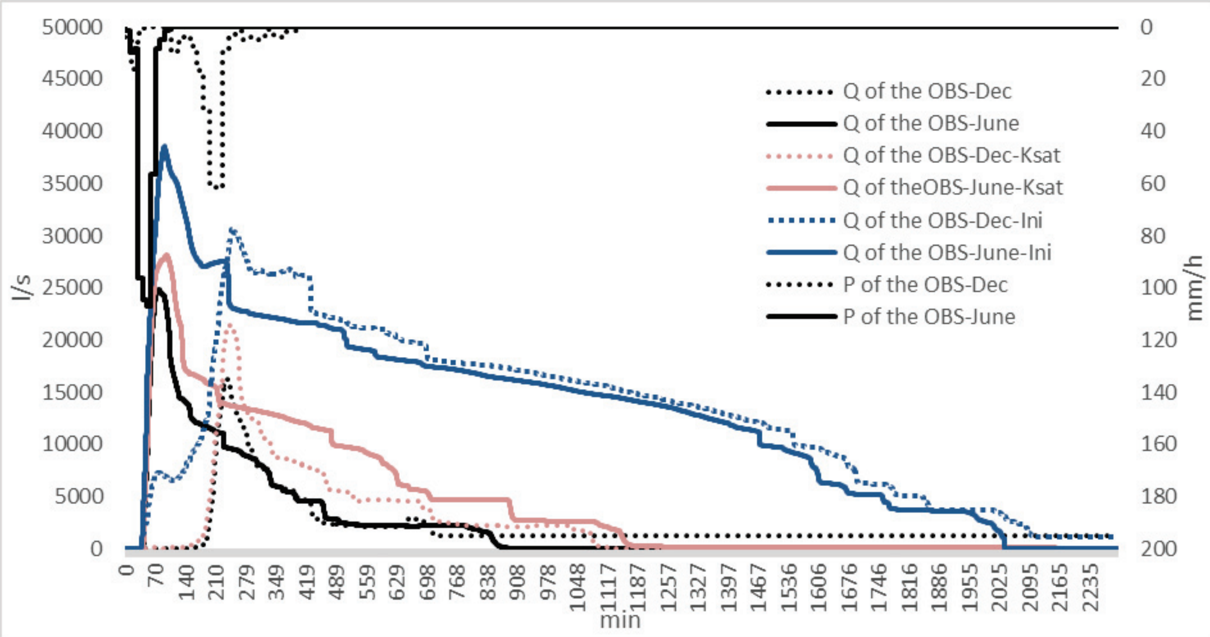

Figure 5.6: : Hydrograph at the main outlet of simulations usning 25June and 15December. The left axis show the precipitation intensity (l/s) while the right axis shows the discharge(mm/h).

5.5. OpenLISEM performance

During the field survey, the main aim was to get information on highest flood depth and longest duration of floods that the local population experienced along different transects in the floodplain. The measured flood depths were compared with all simulated flood depths and durations. The simulated flood depths and durations were extracted to surveyed location in Figure 3.3. The comparison used a simple lineal regression (Andy, 2009). The results are shown in Table 5.2, Figure 5.7 and the table of Appendix 7.7. The level of agreement between simulated results and duration reported by the population was very poor, inexistent in most of the simulations. Flood duration reported by respondents were probably more subjective and unreliable (Appendix 7.5).

	Question
WRF	-0.01
WRF-Ptot	-0.04
WRF-Imax	0.34
WRF-homo	-0.05
WRF-Ptot-homo	-0.08
WRF-Imax-homo	0.35
OBS-June	0.38
OBS-June-Ksat	0.38
OBS-June-Ini	0.34
OBS-Dec	-0.09
OBS-Dec-Ksat	0.36
OBS-Dec-Ini	0.35

Table 5.2: Pearson correlation between simulated flood depth (m) and measured flood depth (m).

The simulated depth showed some level of agreements with measured flood depth. In WRF-Imax, WRF-Imax-homo, OBS-June, OBS-June-Ksat, OBS-June-Ini, OBS-Dec-Ksat, and OBS-Dec-Ini the Pearson correlation was above 0.34 while in other simulations in was even negative (Table 5.2). Simulations with lower correlation predicted almost zero flood depth in the surveyed locations as shown in Figure 5.7 (below 0.4m of flood depth).

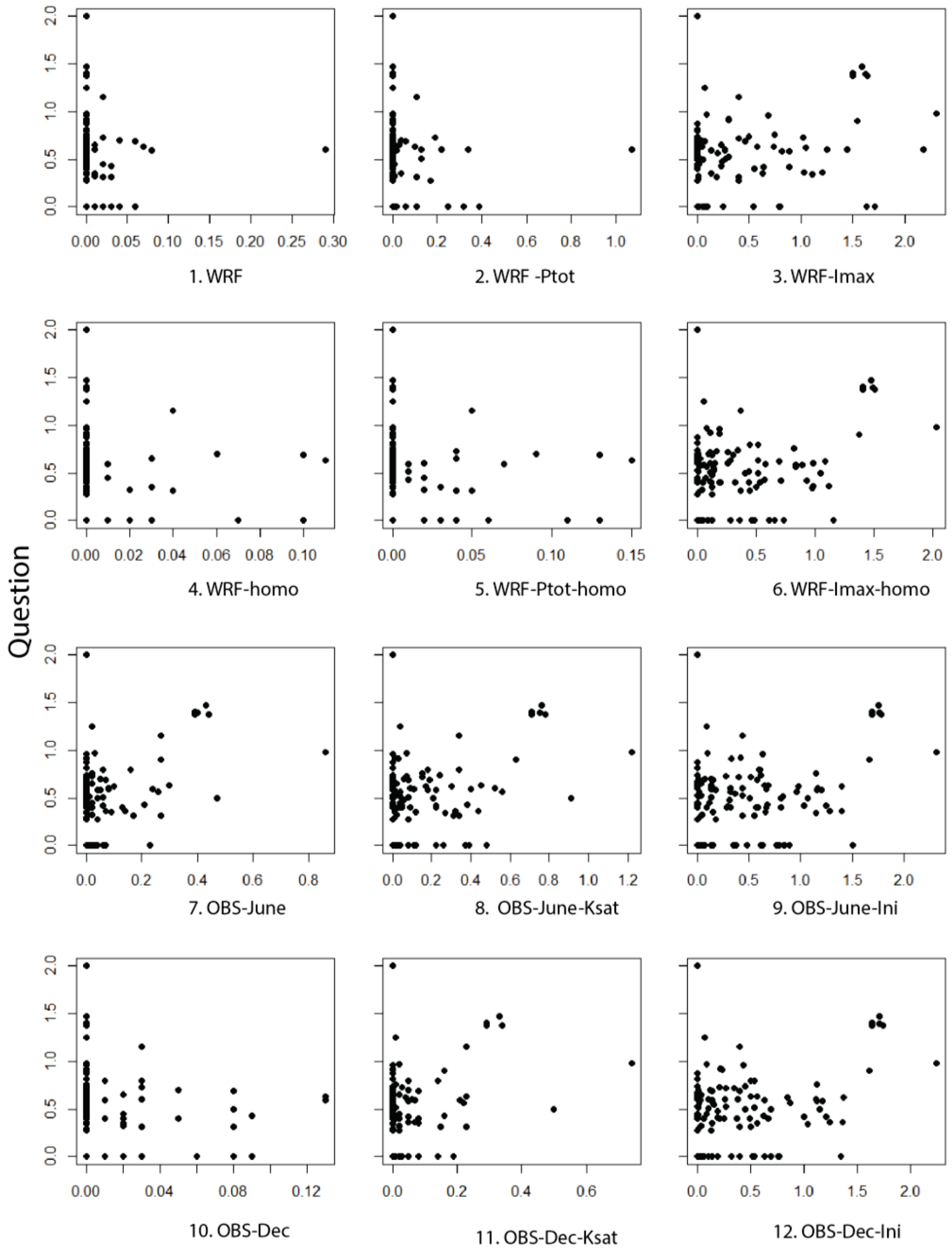

Figure 5.7: Relationship between simulated flood depth and measured depths.

Note that simulations will higher correlation shared in common to have wider flood extents and more areas with deeper flood depth (Figure 5.2 and Figure 5.7). The correlations were low for various probable reasons; the first reason is that the respondents reported the highest water depth they have ever experienced and that they still remember, but the simulation did not use the highest rainfall ever experienced or rainfall that they still remember. The second reason is that acquiring accurate measurements from a participatory approach is very challenging. The third reason is that, the population changes their neighborhood before construction as discussed in section 4.4. However, these changes in local topography were not taken into consideration during simulations. The fourth reason is the resolution of the DEM used (20m). Probably, the resolution was not detailed enough to represent detailed variation of the surveyed locations. The fifth reason is the inaccuracy in drainage dimensions. Inaccurate drainage dimension can lead to erroneous simulation over a location. The last reason is that OpenLISEM simulates floods only from drainage channels. Thus, it is possible to miss floods that occur due to house roof water in undrained location.

The Figure 5.8 shows the local distribution of disagreement in flood depth between simulations and the survey. Figure 5.8 shows only seven simulations more correlated to the survey (WRF-Imax, WRF-Imax-homo, OBS-June, OBS-June-Ksat, OBS-June-Ini, OBS-Dec-Ksat, and OBS-Dec-Ini). In locations shown in red OpenLISEM simulated higher flood depth while the population reported less. Locations in blue the population reported higher flood depth or OpenLISEM did not simulate any flood. In most of the cases, neighbors agree on the flood depth reported as they are a few mixes of disagreement in all images (see the correlation matrix of differences in Appendix 7.7). From Figure 5.8 some areas show a persistent disagreement pattern which can be related to errors in drainage inputs, local topography, respondents who exaggerated the depth, or simply the need for calibration.

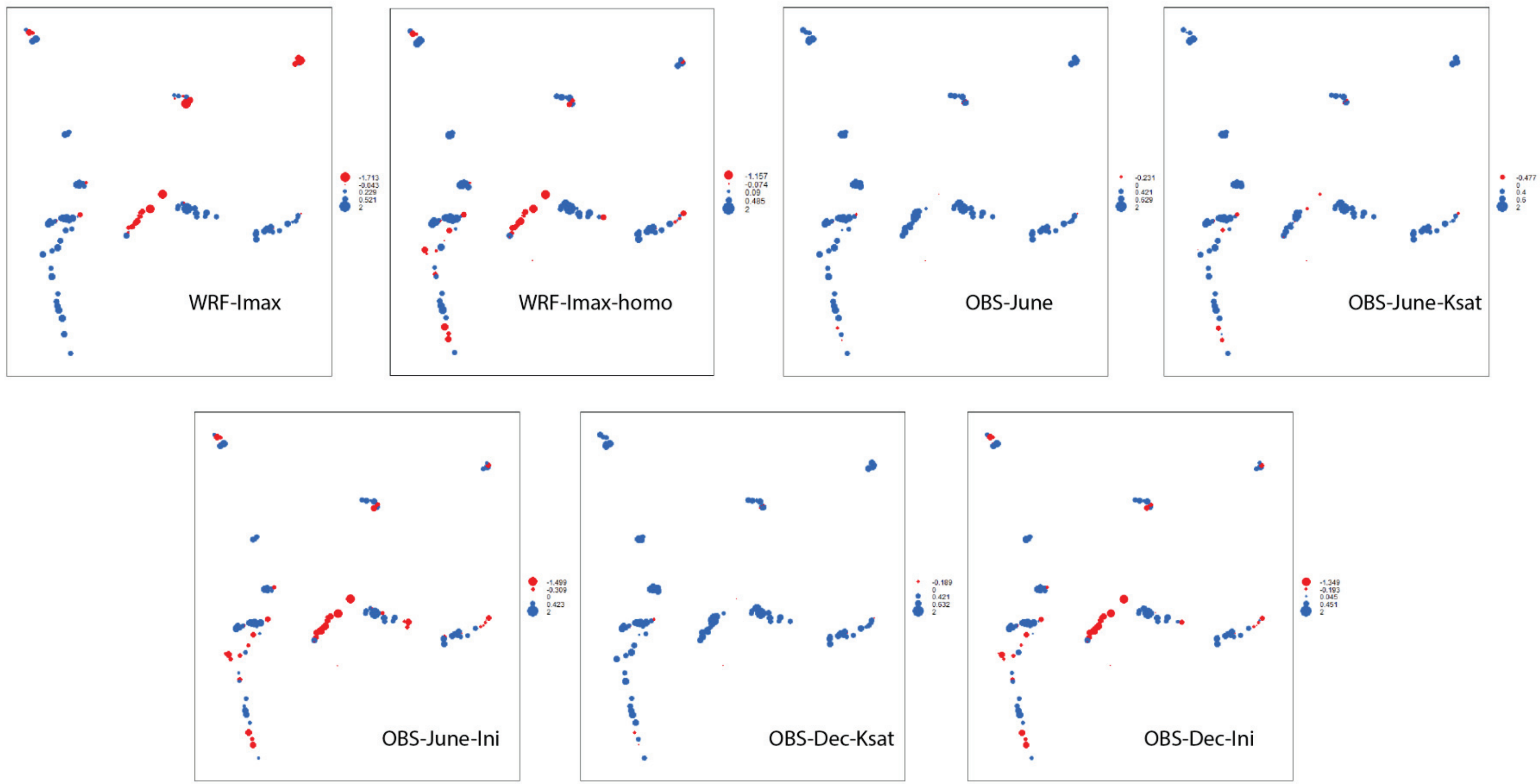

Figure 5.8: Spatial differences between simulations and the survey. Locations in red, OpenLISEM simulated higher values that have reported the population while areas in blue OpenLISEM simulated lower flood depth that reported the population. The range of differences is; for WRF-Imax (-1.7 to 2), WRF-Imax-homo(-1.2 to 2), OBS-June (-0.2 to 2), OBS-June-Ksat (-0.5 to 2), OBS-June-Ini (-1.5 to 2), OBS-Dec-Ksat (-0.2, 2), and OBS-Dec-Ini (-0.3 to 2).

6. CONCLUSION AND RECOMMENDATION

The main objective was to analyse rainfall properties of Lubigi catchment and to integrate spatial and temporal variability of rainfall data in a flood model and to analyse the effects on flood dynamics. The study area was Lubigi catchment which is highly affected by flash floods every year. From field survey, it became clear that flood evidences are numerous in Lubigi floodplains, Kampala. While some of the population abandons their houses because of floods and move to other areas, there are new settlers coming to live in Lubigi floodplains. People who have been longer in the catchment said to be unaware of flood problem before coming to settle in the floodplain, while recently moved settlers in floodplains were well aware of the existing flood risk. Different coping strategies can be seen in every corner of habited floodplain and different structural measures were adopted. Some people elevate the ground level before the construction of their houses while others will either put a barrier in front of doors or small dyke around houses, and small levee around drainage channels. However, lack of strong integrated flood management measures make any effort made by the population unsuccessful. Integrated flood assessment could provide essential information on the existing flood dynamics.

Analysis of rainfall event characteristics is essential for accurate flood analysis. Previously, ACE (2010)defined a rainfall event in Kampala based on daily values. However, here the 10-15minutes observational records are used to define a rainfall event. Based on Brown et al (1985) a rainfall event was defined as a period. For this research, a rainfall event was considered when it persisted for at least 20 minutes with a total rain depth of more than 3mm and maximum intensity of 4mm/h. Over the period 14May 2012 to 11May 2013, 77 rainfall were identified. The maximum intensity measured was 106.8 mm/h, the maximum duration was 5.5 hours, and the maximum rainfall depth event was 66.2mm. Lubigi catchment counted more rainfall events in the afternoon with shorter duration while longer rainfall events mainly occured in the morning. The total rainfall depth was strongly related ($R = 0.79$) to the maximum intensity than it was to the total duration ($R=0.61$). Two observed rainfall events with a two years return probability were identified, which are used to analyse the effect of spatial variable rainfall and of initialisation conditions on the flood dynamics. The OpenLISEM simulations of these events showed different intensities and duration can lead to totally different flood dynamics. For that, the characterisation of rainfall events should not be based on daily but sub-daily event using high temporal resolution. Moreover, rainfall event analysis should not focus only on the total rainfall depth, but also on the probability of return of different rainfall intensities and durations.

Spatio-temporal variable rainfall shows the true nature of rainfall field and can lead to better estimates of flood experienced over an area. The WRF model simulated the rainfall characteristics at a 1km spatial and 10-minute temporal resolution for the period 23 June to 29June 2012. The WRF rainfall was not in agreement with local ground measurements in amount, space, and time distribution of intensities and amounts. However, WRF provides rainfall information on locations where no measurements are available, which could be very valuable for flood dynamics. This is the first attempt to incorporate spatial and temporal variable WRF rainfall in OpenLISEM flood analysis. The simulated rain event on 27 June was characterized by a high intensity and amount over the northern part of the catchment. This high intensity did not move over the catchment but stay mainly in the north.

As expected, simulations using spatial variable rainfall resulted in different flood properties compared to the use of homogeneous rainfall (P. Arnaud et al., 2002; Faurès et al., 1995). The differences can be seen in infiltration, runoff, discharge, hydrograph shape, flood depth, and flood extents. It was evident that the use of homogeneous rainfall can lead to overestimation or underestimation of hydrological processes over ungauged locations. When homogeneous rainfall is used, the entire catchment responds at the same time and all water from the side valleys accumulates in the central valley roughly at the same moment. This was not the case when a spatio-temporal variable rainfall is used. With the present simulations, it is hard to split the effects temporal from spatial variable rainfall. Higher rainfall intensities stayed in the north of the catchment. More simulations with OpenLISEM using calibrated rainfall fields and analysis with the multiple WRF events is needed to determine the impact of spatial variability in rainfall on the Lubigi catchment. Different WRF simulations should be used in the future and over different catchments in order to test the effects on flood dynamics depending on the spatio-temporal movement or location of higher intensities. Furthermore, WRF model is not the only source of spatio-temporal rainfall. In the coming future, researchers can test the use of satellite and radar data in flood modeling as alternative sources of spatio-temporal rainfall.

Flood dynamics of Lubigi catchment depends on rainfall event properties and soil hydraulics conditions. Flood simulations based on rainfall events of shorter duration but with high intensities led to higher peak discharge, total discharge, flood volume, and wider flooded area. This was not the case for flood simulation using a rainfall event of same rainfall depth but of different intensities and duration. The rainfall event of low intensities contributed more to infiltration than to runoff, even when half reduced the hydraulic conductivity of the soils. It was evident that the initial soil condition are highly important for better flood analysis in Lubigi catchment especially for the rainfall of higher intensities. See the effect of initial soil moisture content, in the future, the effect of two or more consecutive rainfall events in flood dynamics in Lubigi should be analysed.

The OpenLISEM simulations were to reasonable level in agreement with flood measures from respondents. The results were compared to what the local population remembered to be the highest flood depth. This comparison might be biased, as the rainfall events used in the simulation were not the most extreme ever experienced in the catchment. In some places, the population reported higher/less flood depth compared to the simulated. The reasons are numerous, but some are important to be highlighted. First, OpenLISEM do not simulate floods in places without drainages, second the resolution of the DEM used can miss the detailed variations of topography, the third is that the population have been modifying local topography as residents try to cope with floods, the fourth is that acquiring accurate measurements from a participatory approach is very challenging. Thus, the calibration of OpenLISEM to an observed flood extent or depth is essential to validate the model accuracy in space. More development of the software is also needed so that the simulation of flood in undrained places became possible, also to reduce errors in mass balance.

LIST OF REFERENCES

Abebe, G. A. (2013). *Quantifying urban growth pattern in developing countries using remote sensing and spatial metrics : a case study in Kampala, Uganda.* University of Twente Faculty of Geo-Information and Earth Observation (ITC), Enschede. Retrieved from http://www.itc.nl/library/papers_2013/msc/upm/abebe.pdf

ACE. (2010). Kampala drainage master plan: Engineering design review and update report.

Alkema, D. (2007). *Simulating floods : on the application of a 2D hydraulic model for flood hazard and risk assessment.* (147), ITC, Enschede. Retrieved from http://www.itc.nl/library/papers_2007/phd/alkema.pdf

Andy, F. (2009). *Discovering statistics using SPSS* (3 ed.): Sage.

Arcement, G. J. J., Schneider, V. R., & USGS. (1984). *Guide for Selecting Manning's Roughness Coefficients for Natural Channels and Flood Plains*. USA: United States Geological Survey: WSP2339.

Arnaud, P., Bouvier, C., Cisneros, L., & Dominguez, R. (2002). Influence of rainfall spatial variability on flood prediction. *Journal of Hydrology, 260*(1–4), 216-230. doi: http://dx.doi.org/10.1016/S0022-1694(01)00611-4

Arnaud, P., Lavabre, J., Fouchier, C., Diss, S., & Javelle, P. (2011). Sensitivity of hydrological models to uncertainty in rainfall input. *Hydrological Sciences Journal, 56*(3), 397-410. doi: 10.1080/02626667.2011.563742

Ba, M. B., & Nicholson, S. E. (1998). Analysis of convective activity and its relationship to the rainfall over the rift valley lakes of east Africa during 1983–90 using the meteosat infrared channel. *Journal of Applied Meteorology, 37*(10), 1250-1264. doi: 10.1175/1520-0450(1998)037<1250:AOCAAI>2.0.CO;2

Bamford, T. B., Bamford, D. J., Lai, R. H. H., & Martin, N. (2008). *Understanding the complexities of urban flooding through integrated modeling.* Paper presented at the 11th International conference of urban flooding through integrated modelling.

Bates, P. D., & Hervouet, J. M. (1999). A new method for moving-boundary hydrodynamic problems in shallow water. *Proceedings of the Royal Society of London Series a-Mathematical Physical and Engineering Sciences, 455*(1988), 3107-3128.

Berne, A., Delrieu, G., Creutin, J.-D., & Obled, C. (2004). Temporal and spatial resolution of rainfall measurements required for urban hydrology. *Journal of Hydrology, 299*(3–4), 166-179. doi: http://dx.doi.org/10.1016/j.jhydrol.2004.08.002

Bivand, R. S., Pebesma, E. J., & Gomez-Rubio, V. (2013). *Applied spatial data analysis with R.* : Springer.

Bracken, L. J., Cox, N. J., & Shannon, J. (2008). The relationship between rainfall inputs and flood generation in south–east Spain. *Hydrological Processes, 22*(5), 683-696. doi: 10.1002/hyp.6641

Brath, A., & Montanari, A. (2000). The effects of the spatial variability of soil infiltration capacity in distributed flood modelling. *Hydrological Processes, 14*(15), 2779-2794. doi: 10.1002/1099-1085(20001030)14:15<2779::AID-HYP91>3.0.CO;2-X

Brody, S. D., Zahran, S., Highfield, W. E., Grover, H., & Vedlitz, A. (2008). Identifying the impact of the built environment on flood damage in Texas. *Disasters, 32*(1), 1-18. doi: 10.1111/j.1467-7717.2007.01024.x

Brown, B. G., Katz, R. W., & Murphy, A. H. (1985). Exploratory Analysis of Precipitation Events with Implications for Stochastic Modeling. *Journal of Climate and Applied Meteorology, 24*(1), 57-67. doi: 10.1175/1520-0450(1985)024<0057:EAOPEW>2.0.CO;2

Burns, D., Vitvar, T., McDonnell, J., Hassett, J., Duncan, J., & Kendall, C. (2005). Effects of suburban development on runoff generation in the Croton River basin, New York, USA. *Journal of Hydrology, 311*(1–4), 266-281. doi: http://dx.doi.org/10.1016/j.jhydrol.2005.01.022

Castillo, V. M., Gómez-Plaza, A., & Martínez-Mena, M. (2003). The role of antecedent soil water content in the runoff response of semiarid catchments: a simulation approach. *Journal of Hydrology, 284*(1–4), 114-130. doi: http://dx.doi.org/10.1016/S0022-1694(03)00264-6

De Roo, A. P. J., Wesseling, C. G., & Ritsema, C. J. (1996). LISEM: a single-event physically based hydrological and soil erosion model for drainage basins. I: Theory, input and output. *Hydrological Processes, 10*(8), 1107-1117. doi: 10.1002/(SICI)1099-1085(199608)10:8<1107::AID-HYP415>3.0.CO;2-4

Delestre, O., Cordier, S., James, F., & Darboux, F. (2009). Simulation of rain-water overland flow. http://www.univ-orleans.fr/mapmo/soft/FullSWOF/
Di Baldassarre, G., Montanari, A., Lins, H., Koutsoyiannis, D., Brandimarte, L., & Bloschl, G. (2010). Flood fatalities in Africa: From diagnosis to mitigation. *Geophysical Research Letters, 37*. doi: 10.1029/2010gl045467
Douglas, I., Alam, K., Maghenda, M., Mcdonnell, Y., Mclean, L., & Campbell, J. (2008). Unjust waters: climate change, flooding and the urban poor in Africa. *Environment and Urbanization, 20*(1), 187-205. doi: 10.1177/0956247808089156
Efstathiou, G. A., Zoumakis, N. M., Melas, D., Lolis, C. J., & Kassomenos, P. (2013). Sensitivity of WRF to boundary layer parameterizations in simulating a heavy rainfall event using different microphysical schemes. Effect on large-scale processes. *Atmospheric Research, 132–133*(0), 125-143. doi: http://dx.doi.org/10.1016/j.atmosres.2013.05.004
Ettema, J.). [WRF model rainfall simulation data].
Faurès, J.-M., Goodrich, D. C., Woolhiser, D. A., & Sorooshian, S. (1995). Impact of small-scale spatial rainfall variability on runoff modeling. *Journal of Hydrology, 173*(1–4), 309-326. doi: http://dx.doi.org/10.1016/0022-1694(95)02704-S
Finaud-Guyot, P., Delenne, C., Guinot, V., & Llovel, C. (2011). 1D–2D coupling for river flow modeling. *Comptes Rendus Mécanique, 339*(4), 226-234. doi: http://dx.doi.org/10.1016/j.crme.2011.02.001
Gallus, W. A., & Bresch, J. F. (2006). Comparison of Impacts of WRF Dynamic Core, Physics Package, and Initial Conditions on Warm Season Rainfall Forecasts. *Monthly Weather Review, 134*(9), 2632-2641. doi: 10.1175/MWR3198.1
Gareth, P., & Sylvain, N. (2007). Use of computer models of flood inundation to facilitate communication in flood risk management. *Environmental Hazards, 7*(2), 106-114. doi: http://dx.doi.org/10.1016/j.envhaz.2007.07.006
Gregory, J. H., Dukes, M. D., Jones, P. H., & Miller, G. L. (2006). Effect of urban soil compaction on infiltration rate. *Journal of Soil and Water Conservation, 61*(3), 117-124.
Gruber, A., & Lezivanni, V. (2008). Assessment of global precipitation products.
Haile, A. T. (2010). *Rainfall variability and estimation for hydrologic modeling.* (PhD), University of Twente/ITC, Enschede.
Haile, A. T., Rientjes, T. H. M., Habib, E., Jetten, V., & Gebremichael, M. (2011). Rain event properties at the source of the Blue Nile River. *Hydrol. Earth Syst. Sci., 15*(3), 1023-1034. doi: 10.5194/hess-15-1023-2011
Hall, J. W., Meadowcroft, I. C., Sayers, P. B., & Bramley, M. E. (2003). Integrated Flood Risk Management in England and Wales. *Natural Hazards Review, 4*(3), 126-135. doi: 10.1061/(asce)1527-6988(2003)4:3(126)
Hessel, R. (2005). Effects of grid cell size and time step length on simulation results of the Limburg soil erosion model (LISEM). *Hydrological Processes, 19*(15), 3037-3049. doi: 10.1002/hyp.5815
Hollis, G. E. (1975). Effect of urbanization on floods of different recurrence interval. *Water Resources Research, 11*(3), 431-435. doi: 10.1029/WR011i003p00431
Horritt, M. S., & Bates, P. D. (2002). Evaluation of 1D and 2D numerical models for predicting river flood inundation. *Journal of Hydrology, 268*(1–4), 87-99. doi: http://dx.doi.org/10.1016/S0022-1694(02)00121-X
Jetten, V. G. (2013a). *A brief guide to openLISEM.*
Jetten, V. G. (2013b). OpenLISEM: a spatial model for runoff, flood and erosion. Retrieved 17th August, 2013, from http://blogs.itc.nl/lisem/
Jha, A. K., Bloch, R., & Lamond, J. (2012). *Cities and flooding: a guide to integrated flood management.* Washington: The World Bank.
Jongman, B., Ward, P. J., & Aerts, J. C. J. H. (2012). Global exposure to river and coastal flooding: Long term trends and changes. *Global Environmental Change, 22*(4), 823-835. doi: http://dx.doi.org/10.1016/j.gloenvcha.2012.07.004
Jonkman, S. N. (2005). Global Perspectives on Loss of Human Life Caused by Floods. *Natural Hazards, 34*(2), 151-175. doi: 10.1007/s11069-004-8891-3
Kidd, C. (2001). Satellite rainfall climatology: a review. *International Journal of Climatology, 21*(9), 1041-1066. doi: 10.1002/joc.635

Kundzewicz, Z. W. (1999). Flood protection - sustainability issues. *Hydrological Sciences Journal-Journal Des Sciences Hydrologiques, 44*(4), 559-571. doi: 10.1080/02626669909492252
Kundzewicz, Z. W. (2002). Non-structural flood protection and sustainability. *Water International, 27*(1), 3-13.
Kundzewicz, Z. W., & Takeuchi, K. (1999). Flood protection and management: quo vadimus? *Hydrological Sciences Journal, 44*(3), 417-432. doi: 10.1080/02626669909492237
Kusumastuti, D. I., Struthers, I., Sivapalan, M., & Reynolds, D. A. (2007). Threshold effects in catchment storm response and the occurrence and magnitude of flood events: implications for flood frequency. *Hydrol. Earth Syst. Sci., 11*(4), 1515-1528. doi: 10.5194/hess-11-1515-2007
Li, G.-F., Xiang, X.-Y., Tong, Y.-Y., & Wang, H.-M. (2013). Impact assessment of urbanization on flood risk in the Yangtze River Delta. *Stochastic Environmental Research and Risk Assessment, 27*(7), 1683-1693. doi: 10.1007/s00477-013-0706-1
Lin, B., Wicks, J. M., Falconer, R. A., & Adams, K. (2006). Integrating 1D and 2D hydrodynamic models for flood simulation. *Proceedings of the Institution of Civil Engineers-Water Management, 159*(1), 19-25.
Ly, S., Charles, C., & Degré, A. (2011). Geostatistical interpolation of daily rainfall at catchment scale: the use of several variogram models in the Ourthe and Ambleve catchments, Belgium. *Hydrol. Earth Syst. Sci., 15*(7), 2259-2274. doi: 10.5194/hess-15-2259-2011
Maidment, R. I., Grimes, D. I. F., Allan, R. P., Greatrex, H., Rojas, O., & Leo, O. (2013). Evaluation of satellite-based and model re-analysis rainfall estimates for Uganda. *Meteorological Applications, 20*(3), 308-317. doi: 10.1002/met.1283
Matagi, S. V. (2002). Some issues of environmental concern in Kampala, the capital city of Uganda. *Environmental Monitoring and Assessment, 77*(2), 121-138. doi: 10.1023/A:1015860820467
Mignot, E., Paquier, A., & Haider, S. (2006). Modeling floods in a dense urban area using 2D shallow water equations. *Journal of Hydrology, 327*(1–2), 186-199. doi: http://dx.doi.org/10.1016/j.jhydrol.2005.11.026
Musgrave, W. F. (1985). Flood Damage Mitigation: A Review of Structural and Nonstructural Measures and Alternative Decision Frameworks. *Water Resources Research, 21*(4), 411-424. doi: 10.1029/WR021i004p00411
NEMA. (2008). State of environment: Report for Uganda. Kampala.
NEMA. (2009). *Atlas of our changing environment*. Kampala.
NEMA. (2010). State of environment: Report for Uganda. Kampala.
Nirupama, N., & Simonovic, S. (2007). Increase of Flood Risk due to Urbanisation: A Canadian Example. *Natural Hazards, 40*(1), 25-41. doi: 10.1007/s11069-006-0003-0
Nkurunziza, E. (2008). Understanding informal urban land access processes from a legal pluralist perspective: The case of Kampala, Uganda. *Habitat International, 32*(1), 109-120. doi: http://dx.doi.org/10.1016/j.habitatint.2007.08.004
Oyoo, R., Leemans, R., & Mol, A. P. (2013). The determination of an optimal waste management scenario for Kampala, Uganda. *Waste Management & Research, 31*(12), 1203-1216. doi: 10.1177/0734242x13507307
Pebesma, E. (2013). Spatial and spatio-temporal geostatistical modelling, prediction and simulation.
Pennelly, C., Reuter, G., & Flesch, T. (2014). Verification of the WRF model for simulating heavy precipitation in Alberta. *Atmospheric Research, 135–136*(0), 172-192. doi: http://dx.doi.org/10.1016/j.atmosres.2013.09.004
Philippon, N., Camberlin, P., & Fauchereau, N. (2002). Empirical predictability study of October–December East African rainfall. *Quarterly Journal of the Royal Meteorological Society, 128*(585), 2239-2256. doi: 10.1256/qj.01.190
Pitt, R., Chen, S. E., Clark, S. E., Swenson, J., & Ong, C. K. (2008). Compaction's impacts on urban storm-water infiltration. *Journal of Irrigation and Drainage Engineering-Asce, 134*(5), 652-658. doi: 10.1061/(asce)0733-9437(2008)134:5(652)
Roger, Z. (2012). World disaster report 2012: Focus on forced migration and displacement. Geneva.
Rossiter, D. G. (2014). Kampala soils: Hydraulic soil properties.
Segond, M.-L., Wheater, H. S., & Onof, C. (2007). The significance of spatial rainfall representation for flood runoff estimation: A numerical evaluation based on the Lee catchment, UK. *Journal of Hydrology, 347*(1–2), 116-131. doi: http://dx.doi.org/10.1016/j.jhydrol.2007.09.040

Shrestha, A. B., Chapagain, P. S., & Thapa, R. (2011). *Flash flood risk management: a training of trainers manual: also as e-book*. Kathmandu: International Centre for Integrated Mountain Development (ICIMOD).

Skamarock, W. C., Klemp, J. B., Dudhia, J., Gill, D. O., Barker, D. M., Duda, M. G., . . . Powers, J. G. (2008). *A description of the Advanced Research WRF Version 3*. Colorado.

Stelling, G. S., & Verwey, A. (2006). Numerical Flood Simulation *Encyclopedia of Hydrological Sciences*: John Wiley & Sons, Ltd.

Tapsell, S. M., Penning-Rowsell, E. C., Tunstall, S. M., & Wilson, T. L. (2002). Vulnerability to flooding: health and social dimensions. *Philosophical Transactions of the Royal Society of London Series a-Mathematical Physical and Engineering Sciences, 360*(1796), 1511-1525. doi: 10.1098/rsta.2002.1013

Tingsanchali, T. (2012). Urban flood disaster management. *Procedia Engineering, 32*(0), 25-37. doi: http://dx.doi.org/10.1016/j.proeng.2012.01.1233

UN-Habitat. (2007). *Situation Analysis of Informal Settlements in Kampala*. Nairobi: United Nations Human Settlement Programme.

Van Mullem, J. (1991). Runoff and Peak Discharges Using Green Ampt Infiltration Model. *Journal of Hydraulic Engineering, 117*(3), 354-370. doi: doi:10.1061/(ASCE)0733-9429(1991)117:3(354)

Vermeiren, K., Van Rompaey, A., Loopmans, M., Serwajja, E., & Mukwaya, P. (2012). Urban growth of Kampala, Uganda: Pattern analysis and scenario development. *Landscape and Urban Planning, 106*(2), 199-206. doi: http://dx.doi.org/10.1016/j.landurbplan.2012.03.006

Vojinovic, Z., & Tutulic, D. (2009). On the use of 1D and coupled 1D-2D modelling approaches for assessment of flood damage in urban areas. *Urban Water Journal, 6*(3), 183-199. doi: 10.1080/15730620802566877

WMO. (2006). *Environmental aspect of integrated flood management*. Geneva.

WMO. (2009). *Integrated flood management: Concept paper*. Geneva.

Xie, P., & Arkin, P. A. (1996). Analyses of Global Monthly Precipitation Using Gauge Observations, Satellite Estimates, and Numerical Model Predictions. *Journal of Climate, 9*(4), 840-858. doi: 10.1175/1520-0442(1996)009<0840:AOGMPU>2.0.CO;2

Zehe, E., Becker, R., Bárdossy, A., & Plate, E. (2005). Uncertainty of simulated catchment runoff response in the presence of threshold processes: Role of initial soil moisture and precipitation. *Journal of Hydrology, 315*(1–4), 183-202. doi: http://dx.doi.org/10.1016/j.jhydrol.2005.03.038

7. APPENDICES

Appendix 7.1: An example of questionnaire used during the field survey between 26/9-19/10/2013.

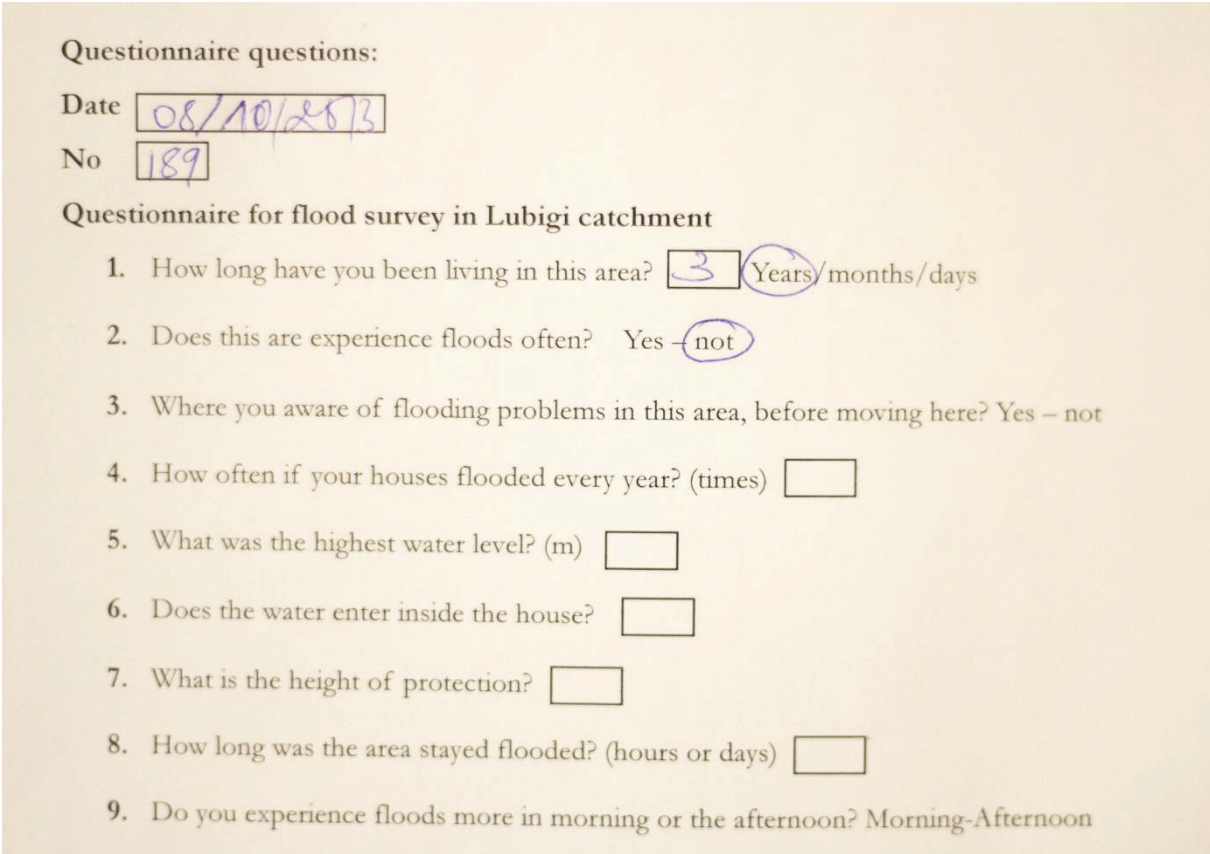

Questionnaire questions:

Date 08/10/2013

No 189

Questionnaire for flood survey in Lubigi catchment

1. How long have you been living in this area? 3 Years/months/days
2. Does this are experience floods often? Yes – not
3. Where you aware of flooding problems in this area, before moving here? Yes – not
4. How often if your houses flooded every year? (times)
5. What was the highest water level? (m)
6. Does the water enter inside the house?
7. What is the height of protection?
8. How long was the area stayed flooded? (hours or days)
9. Do you experience floods more in morning or the afternoon? Morning-Afternoon

Appendix 7.2: A summary of sizes of drainages points measured around Lubigi catchment.

	Class	Min	1st quart.	Median	Mean	3rd quart.	Max
Top width	Primary	3.9	4.5	12	9.005	12	12
	Secondary	1.703	2.6	3.06	3.161	3.5	6.401
	Tertiary	0.48	0.84	1	1.153	1.365	3.29
	Culvert	1	1	1	1.1	1.2	1.5
Bottom width	Primary	3	3.5	10	7.449	10	10
	Secondary	0.8	2	2.05	2.518	3	6
	Tertiary	0.41	0.5	0.662	0.769	1	2.2
	Culvert	1	1	1	1.1	1.2	1.5
Depth	Primary	1.001	1.2	1.6	1.577	1.8	2.2
	Secondary	0.725	1	1.2	1.274	1.5	2.487
	Tertiary	0.5	0.61	0.8	0.820	0.990	1.8
	Culvert	0.9	1	1	1.094	1.2	1.5

Appendix 7.3: WRF model rainfall when Ptot and Imax are calibrated to the measured values. A multiplication factor of 2.142 was used for Ptot calibration while it was 4.343 for Imax.

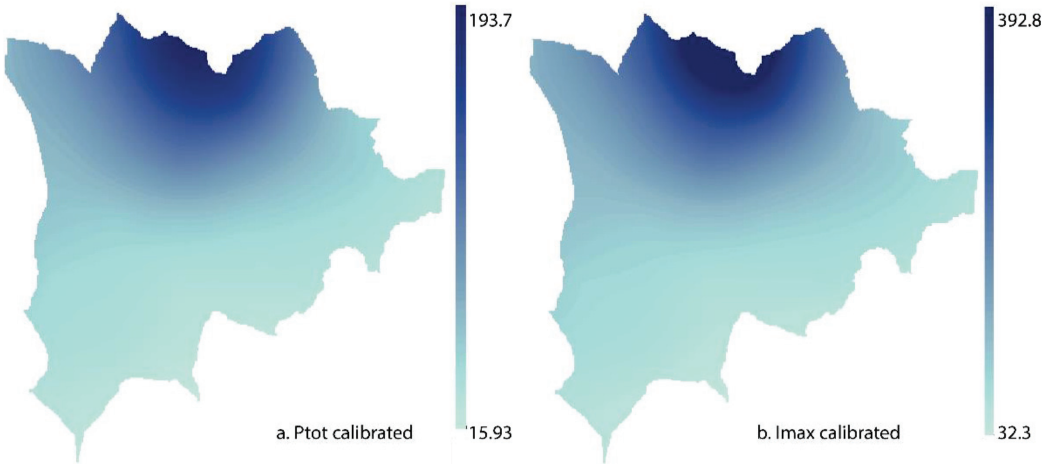

Appendix 7.4: The summary of all rainfall events used in OpenLISEM simulations. The higher values of Ptot, and Imax of WRF rainfall are also highlighted including the spatial average. The spatial averages of 27June WRF rainfalls were later used as homogeneous rainfall.

	27June WRF		WRF Ptot calibrated		WRF Imax calibrated		25-Jun	15-Dec
	High	Average	High	Average	High	Average		
Ptot(mm)	90.9	37.9	193.7	66.2	392.8	134.2	66.2	65.6
Imax(mm/h)	96.3	28.4	168.5	51.2	361.13	106.8	106.8	61.6
Duration(h)	3	3	3	3	3	3	1.5	5.5

Appendix 7.5: Correlation matrix showing the relationship between all simulated flood duration and the results of field survey.

Appendix 7.6: correlation matrix showing the correlation between difference between measured flood depth and the most correlated OpenLISEM floods simulation.

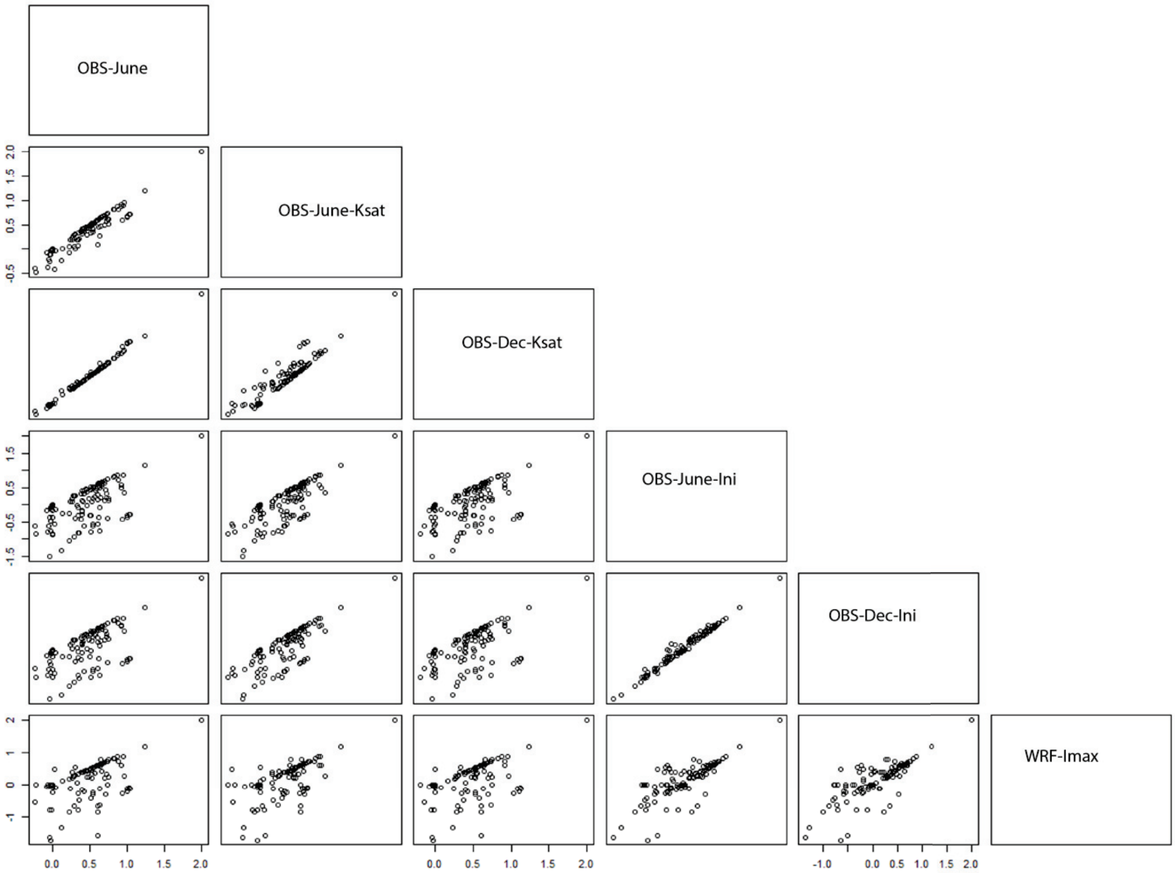

Appendix 7.7: Correlation matrix between different simulations including the outcome of field survey.

	Question	s1	s2	s3	s4	s5	s6	s7	s8	s9	s10	s11	s12
Question	1	-0.01	-0.04	0.34	-0.05	-0.08	0.35	0.38	0.38	0.34	-0.09	0.36	0.35
s1		1	0.80	0.30	0.34	0.42	0.13	0.06	0.20	0.11	0.40	0.08	0.12
s2			1	0.49	0.10	0.18	0.12	-0.03	0.11	0.12	0.13	-0.02	0.12
s3				1	-0.01	0.04	0.77	0.53	0.64	0.77	0.00	0.49	0.79
s4					1	0.92	-0.02	0.17	0.09	-0.05	0.64	0.18	-0.04
s5						1	-0.01	0.19	0.11	-0.04	0.81	0.21	-0.03
s6							1	0.75	0.88	0.98	0.09	0.71	0.99
s7								1	0.93	0.67	0.33	0.99	0.71
s8									1	0.81	0.27	0.91	0.85
s9										1	0.05	0.63	0.99
s10											1	0.36	0.06
s11												1	0.67
s12													1